INRIA

INSTITUT NATIONAL DE RECHERCHE EN INFORMATIQUE ET EN AUTOMATIQUE

Qualitative Simulation of the Nutritional Stress Response in *Escherichia coli*

Delphine Ropers — Hidde de Jong — Michel Page —

Dominique Schneider — Johannes Geiselmann

N° 5412

Décembre 2004

Thème BIO

ISSN 0249-6399 ISRN INRIA/RR--5412--FR+ENG

INRIA
RHÔNE-ALPES

Qualitative Simulation of the Nutritional Stress Response in *Escherichia coli*

Delphine Ropers* , Hidde de Jong* , Michel Page* ,
Dominique Schneider† , Johannes Geiselmann†

Thème BIO — Systèmes biologiques
Projet Hélix

Rapport de recherche n° 5412 — Décembre 2004 — 39 pages

Abstract: In case of nutritional stress, *Escherichia coli* cells abandon their exponentially-growing state to enter a more resistant, non- or slow-growing state termed stationary phase. This growth-phase transition is controlled by a genetic regulatory network integrating various environmental signals. Although *E. coli* is a paradigm of the bacterial world, it is not known how its adaptative response to nutritional conditions emerges from the interactions between the different components of the genetic network. Moreover little quantitative data on kinetic parameters and molecular concentrations are available. To overcome these constraints, we use a qualitative simulation method to model the nutritional stress response network and to simulate the response of *E. coli* cells to nutrient deprivation. Using this method, we are able to capture essential features of the transition between exponential and stationary phase and to make new predictions concerning the system behavior, that are currently under experimental validation.

Key-words: Qualitative modeling and simulation, piecewise-linear differential equations, genetic regulatory networks, nutritional stress response, *Escherichia coli*

* Institut National de Recherche en Informatique et en Automatique, Unité de recherche Rhône-Alpes, Grenoble, France
† Laboratoire Adaptation et Pathogénie des Microorganismes, CNRS UMR 5163, Université Joseph Fourier, Grenoble, France

Unité de recherche INRIA Rhône-Alpes
655, avenue de l'Europe, 38334 Montbonnot Saint Ismier (France)
Téléphone : +33 4 76 61 52 00 —Télécopie +33 4 76 61 52 52

Simulation qualitative de la réponse au stress nutritionnel chez *Escherichia coli*

Résumé : En cas de stress nutritionnel, la bactérie *Escherichia coli* abandonne sa phase de croissance exponentielle pour entrer en phase stationnaire, c'est-à-dire un état physiologique dans lequel les cellules sont plus résistantes et leur croissance est ralentie, voire stoppée. Cette transition entre les deux phases de croissance est contrôlée par un réseau de régulation génique intégrant divers signaux environnementaux. Bien que *Escherichia coli* soit un paradigme dans le monde bactérien, il n'est pas compris à l'heure actuelle comment son adaptation aux conditions nutritionnelles emerge des interactions entre les différents composants du réseau génique. En outre, peu de données quantitatives sur les paramètres cinétiques et les concentrations moléculaires sont disponibles. Afin de surmonter ces contraintes, nous avons employé une méthode de simulation qualitative pour modéliser le réseau de réponse au stress nutritionnel et pour simuler la réponse d'*Escherichia coli* à la privation en nutriments. En utilisant cette méthode, nous avons ainsi pu reproduire les caractéristiques essentielles de la transition entre la phase exponentielle ou stationnaire et nous avons également pu faire des prédictions concernant le comportement du système, lesquelles sont actuellement en cours de validation expérimentale.

Mots-clés : Modélisation et simulation qualitative, équations différentielles linéaires par morceaux, réseaux de régulation génique, réponse au stress nutritionnel, *Escherichia coli*

1 Introduction

In their natural environment, bacteria rarely encounter conditions allowing continuous, balanced growth. While nutrients are available, bacterial populations grow quickly, leading to an exponential increase of their biomass, a state called *exponential phase*. However, upon depletion of an essential nutrient, the bacteria are no longer able to maintain fast growth rates, and the population consequently enters a non- or slow-growth state, called *stationary phase* (figure 1(a)). During the transition from exponential to stationary phase, each individual bacterium develops an ability to survive prolonged periods of starvation and becomes resistant to multiple stresses. For example, some Gram-positive bacteria, like *Bacillus subtilis*, can differentiate into spores [106], whereas *Escherichia coli* and related enteric bacteria undergo other important modifications of their morphology and physiology (figure 1(b)) [50].

When looked at in more detail, the *nutritional stress response* in *E. coli* is a two-stage process involving cascades of molecular events [46]. The first stage is specific to the particular nutrient that is missing. It allows higher-affinity uptake of the limiting nutrient, or the use of an alternative nutrient source. At the same time, development of bacterial motility and chemotaxis increases the probability that bacteria find environmental conditions more appropriate for growth. If induction of this nutrient-specific response remains unsuccessful, in the sense that growth of the cell cannot be resumed, the stress response enters a second stage, characterized by the transition to stationary phase. The stress response induced at this stage is more general, because it is independent of the particular nutrient that is missing or the nature of the stress [47]. It involves numerous morphological and physiological changes, while the cellular metabolism, previously aimed at maximal growth, is reoriented towards a metabolism of maintenance. In addition, a large number of genes are induced whose function it is to provide maximal protection against a variety of stresses [50, 63]. DNA topology is also affected by this process. The DNA, usually supercoiled during exponential phase, becomes relaxed when cells enter stationary phase [9]. The nutritional stress response can be reversed and growth resumed, as soon as nutrients become available again.

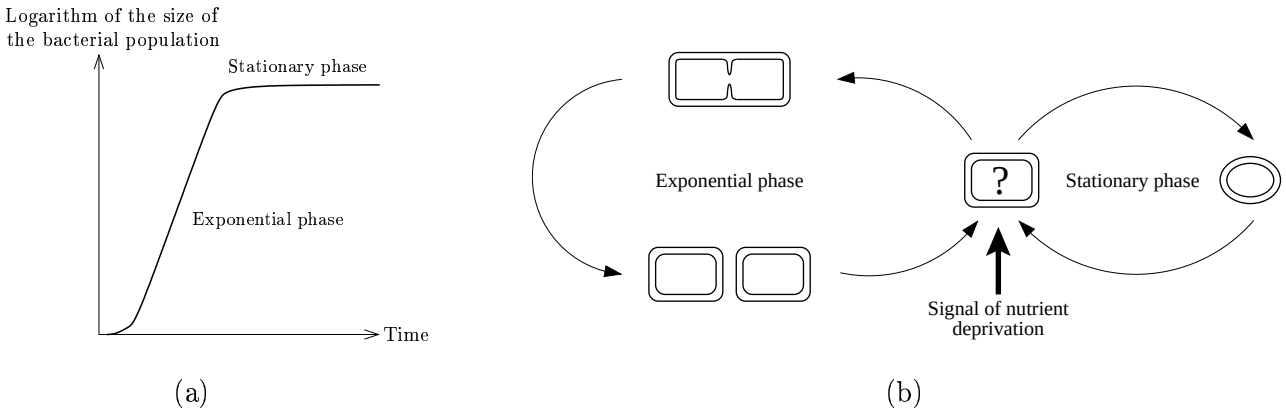

Figure 1: (a) Growth states of a bacterial population: exponential and stationary phase. (b) Nutrient-stress response of bacteria during the transition from exponential to stationary phase.

The morphological and physiological changes of *E. coli* cells underlying the transition of the bacterial population from exponential to stationary phase are determined at the genetic level [19, 20, 46, 52, 102, 108]. The switch in gene expression accompanying the growth-phase transition is controlled by a complex genetic regulatory network integrating various environmental signals [47, 71, 117]. Among the numerous genes, proteins, and metabolites making up this network, a class of pleiotropic transcription factors, called *global regulators*, plays a key role [38]. Global regulators mediate the activation or repression of a large number of genes in response to changes in environmental conditions, such as nutrient

deprivation. Hence, they are able to regulate operons belonging to different metabolic pathways, as well as genes involved in different cellular processes. Many transcription factors have been identified in *E. coli*, but only some of them classify as major global regulators: CRP, IHF, FNR, Fis, Lrp, HNS, and ArcA [69, 71, 103]. These proteins are able to directly modulate the expression of 51% of *E. coli* genes. DNA topology is also considered as a global regulator, since the expression of many genes has been shown to be sensitive to the DNA supercoiling level [44]. The ways in which these global regulators exercise their control are multifarious: they are able to regulate gene expression alone or jointly with other global or specific regulators [71]. They also control the expression of their own genes and the genes encoding their co-regulators through feedback loops that may be highly complex.

The adaptation of *E. coli* cells to new environmental conditions therefore relies on an intricate network of interactions that global regulators establish with other transcription factors and target genes [47, 71, 117]. The ability of the global regulators to activate or inhibit gene expression can be controlled by metabolites, which are usually produced in response to specific environmental perturbations. Due to the joint control of gene expression by the global regulators and their co-regulators, the cell is able to switch sets of target genes on or off in a combinatorial fashion.

The genetic regulatory network controlling the adaptation of the *E. coli* cells during the transition from exponential to stationary phase has been the subject of extensive studies for decades. For example, the mechanism of action of each global regulator is well known, as well as the identity of most of the other transcription factors and target genes involved in the process [12, 19, 38, 46, 71, 88, 97]. However, most studies have focused on only one or a few components of the network and currently no global view exists of the precise functioning of the network as a whole. Computer modeling and simulation tools may help to clarify how the global behavior of this kind of complex system emerges from the local interactions between its components [73]. Indeed, they provide a framework for integrating available biological data at the molecular level and for predicting the behavior of the system under various environmental and physiological conditions. This not only contributes to a better understanding of the role of the different components of the network and their interactions, but also allows the formulation of hypotheses about missing components and interactions, which may guide further experimentation.

A wide variety of mathematical formalisms for describing genetic network dynamics exists, giving rise to qualitative or quantitative, discrete or continuous, stochastic or deterministic models [21]. The most widely-used approach is based on ordinary differential equations (ODEs) and has a solid foundation in the kinetic theory of biochemical reactions. However, the use of chemical kinetics requires precise knowledge of biochemical reaction mechanisms, as well as quantitative information about molecular concentrations and kinetic parameters. Even in the case of well-studied systems, like the *E. coli* stress response network, this level of knowledge is almost never obtained. A way to deal with this problem is to use a special class of piecewise-linear (PL) differential equation models, originally proposed by Glass and Kauffman [34]. The state variables in the PL models correspond to the concentrations of the proteins encoded by genes in the network, while the differential equations describe the influence of each regulatory protein on the synthesis and degradation of other network components. The models use a simplified description of the regulatory interactions in terms of step functions, motivated by the nonlinear, switch-like character of the interactions involved in gene expression. In addition, PL differential equations can be qualitatively analyzed, which circumvents the problem that quantitative information is usually lacking [24, 34].

In order to better understand how *E. coli*'s growth-phase transition emerges from the interactions between the global regulators of transcription, we have modeled and simulated the behavior of the nutritional stress response network. Because quantitative data are usually absent, we have used a qualitative modeling and simulation method based on the PL models of genetic regulatory networks, introduced by de Jong *et al.* [24]. This approach has been successfully applied to the analysis of the regulatory networks controlling the initiation of sporulation in *B. subtilis* [22] and quorum sensing in

Pseudomonas aeruginosa [113]. Our model is based on a system of six piecewise-linear differential equations, representing the evolution of the concentration of key global regulators in the nutritional stress response network. Simulations of the adaptation of *E. coli* growth in response to a nutritional stress have been performed by means of the publicly-available software tool Genetic Network Analyzer (GNA) [23].

The predictions thus obtained display two interesting features. First, the reorganization of the gene expression pattern during the transitions between the exponential and stationary-growth phases relies on the fine-tuned control of the expression and activity of the global regulators. In particular, the switch in the expression of *fis* and *crp* is crucial for this process. Second, oscillations of protein concentrations are observed after a nutrient upshift, due to the homeostatic control of DNA topology. From a more general point of view, our mathematical model connects functional modules in the nutritional stress network – that have been usually studied in isolation –, and shows how the global behavior of adaptation of the cells to their environment emerges from local interactions at the molecular level inside and between modules.

In the next section, we review our current knowledge about the network of interactions controlling the nutritional stress response in *E. coli*. Section 3 summarizes the qualitative modeling and simulation approach that has been used to analyze the nutritional stress response network. In sections 3 and 4 we present a qualitative PL model of the network of key global regulators and the functional modules in which they are involved. The results of qualitative simulation are presented in section 5, followed by a discussion of the biological implications of these results in the concluding section of the paper.

2 The nutritional stress response network

Bacterial habitats are continuously perturbed by changes in, for example, temperature, pH, pressure, and nutrient availability. In order to survive, bacteria have to sense such modifications and respond to them by adapting the expression of regulatory proteins controlling the cellular morphology and physiology [50, 63]. In other words, the fitness of bacterial species depends on their ability to make decisions in response to a variety of environmental perturbations. In the case of *E. coli* cells, the nutritional stress response is a particularly important growth decision, because the bacteria have to decide between growing exponentially - and therefore reproducing - or slowing down growth and entering stationary phase.

On the molecular level, the transition from exponential to stationary phase is accompanied by a wide-ranging reorganization of the morphology, physiology, and gene expression of the individual cells, allowing the bacteria to become more resistant to the hostile environmental conditions [47, 117]. As *E. coli* is a paradigm of the bacterial world, the molecular processes underlying this adaptation to nutrient availability have been extensively studied [46, 47, 50, 63, 97]. In particular, a complex genetic regulatory network has been shown to be responsible for the growth-phase transition. Key players in this genetic network - the major global regulators of transcription (CRP, IHF, FNR, FIS, Lrp, HNS, and ArcA) and DNA supercoiling - as well as their interactions have been identified [71]. However, we still lack an understanding of the functioning of the network as a whole. The intricate structure of interactions of the network makes it difficult to gain an intuitive comprehension of the dynamics of the system. This shortcoming motivates the recourse to modeling opted for in this report.

In order to model the nutritional stress response in *E. coli*, we have chosen to advance by a modular approach, based on evidence that the functioning of genetic regulatory networks arises from subnetworks with a specific role that are connected to each other [43]. These modules are defined by three global regulators (CRP, Fis, and DNA topology), one input (a signal of nutritient deprivation), and one output (the stable RNA concentration). In order to fill in the molecular details, we have used data from the extensive literature on the nutritional stress response in *E. coli* and computerized resources such as EcoCyc [58, 59] and RegulonDB [98]. Fig. 2 depicts the components of this network

and their interactions, using conventions proposed by Kohn [62]. The network structure is organized in four interconnected modules that are described below.

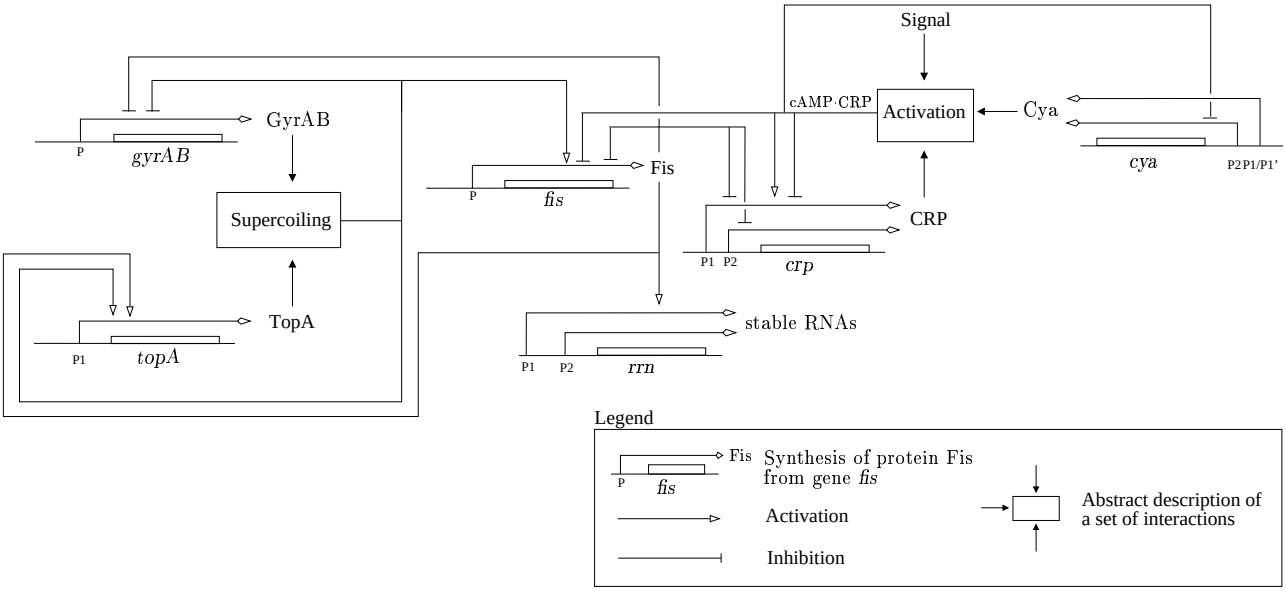

Figure 2: Network of key genes, proteins, and regulatory interactions involved in the nutritional stress network in *Escherichia coli*. The contents of the box 'activation' and 'supercoiling' are detailed in the text. Graphical conventions [62] are described in the legend.

The first module concerns the input of the system. In adaptation processes of the kind considered here, the relationship between sensing external stimuli and expressing appropriate genes involves first of all transporters and signal-transduction mechanisms, driving protein activation and metabolite production. In *E. coli*, the lack of nutrients is transduced by the activation of the adenylate cyclase enzyme (Cya) and the subsequent production of cAMP, a small metabolite that binds the dimeric form of the protein CRP (cAMP receptor protein) [97]. This process involves the same proteins that compose the phosphotransferase system (PTS), responsible for the regulation of the transport of sugars [88]. The PTS senses the lack of nutrients and sends the information to other cellular processes through a cascade of phosphorylation reactions triggering the activation of adenylate cyclase. The enzyme's active form is able to efficiently produce cAMP from ATP [97]. Because in this paper we focus on the effect of the signal on the adaptation of the cell to adverse growth conditions, the PTS signal-transduction pathway will not be modeled in detail (some examples of models of this system can be found in the literature [30, 64, 93, 109]). Instead, we simplify the signal-transduction pathway by considering a signal indicating a lack of nutrients (abbreviated to Signal), that directly activates Cya under nutritional stress conditions.

The second network module comprises three genes: *crp*, *cya*, and *fis*. The CRP global regulator is the target of the signal-transduction pathway: as soon as the cAMP metabolite is produced, it binds CRP, thus activating the transcription factor and allowing it to regulate gene expression [42, 68]. The cAMP·CRP complex controls the expression of two kinds of genes. The first category is composed of genes directly involved in the adaptative response to nutritient deprivation: for example, it activates the synthesis of catabolic enzymes, thus amplifying the potential of the cells to make use of alternative sources of carbon and thereby escape carbon limitation [37, 97]. cAMP·CRP also controls the expression of genes involved in changes of cellular morphology and motility. The second category of cAMP·CRP-responsive genes are those encoding global regulators like the proteins Fis and CRP itself [37, 71]. In addition to its autoregulation, the *crp* gene is regulated by Fis [36]. The latter protein is responsible for the control of a large number of genes involved in the cellular metabolism [35], and

is specifically produced at a very high level during exponential phase [6, 10]. Fis and cAMP·CRP mutually repress each other's expression.

The third network module contains genes encoding the proteins GyrAB, TopA, and Fis involved in the control of DNA topology. Bacterial chromosomes in living cells are generally in a negatively-supercoiled rather than relaxed form [25, 86]. Negative supercoiling is an important modulator of all processes involving DNA as a substrate, that is, processes melting, bending, or distorting the molecule. In particular, it influences the transcription of many genes, either by realigning the anchor sites of the RNA polymerase in the promoter region, thus favoring the recognition of the latter by the enzyme, or by facilitating local DNA unwinding, which is required for transcription initiation [44]. The control of DNA supercoiling mainly involves two bacterial topoisomerases [25, 92]. One is a heterodimeric complex, the DNA gyrase GyrAB, composed of the products of the genes *gyrA* and *gyrB*. Whereas GyrAB introduces negative supercoils into the DNA molecule in an ATP-dependent manner, the product of the gene *topA*, the topoisomerase TopA, removes negative supercoils without requiring ATP. Except during growth transitions, the supercoiling level is tightly autoregulated in bacteria. An increase of negative supercoiling by GyrAB is compensated by the activation of *topA* expression, which leads to increased levels of TopA, and thus relaxation of excessive negative supercoiling [9, 44]. Conversely, a decrease in negative supercoiling activates *gyrA* and *gyrB* promoters and thus increases GyrAB production, thereby restoring the physiological level of DNA supercoiling. The protein Fis also takes part in this fine-tuning process of homeostatic control [74], since an increase of negative supercoiling stimulates Fis expression, which represses GyrAB production on the one hand, and stimulates TopA expression on the other hand [100, 101, 111]. Since the genes *gyrA* and *gyrB* encoding GyrAB are regulated in a similar way [100], we will here simplify the discussion and consider the GyrAB complex as the product of a single gene *gyrAB*. Since GyrAB requires ATP for its activity, it is likely that cellular energy also affects DNA topology and therefore controls expression of supercoiling-sensitive genes. However, in this report, we will assume DNA supercoiling to be only dependent on the amounts of GyrAB and TopA.

The last network module controls cellular growth and thus represents the output of the system. It is composed of genes encoding Fis and stable RNAs. The latter are considered as representative of the cell's growth state, since cells growing and dividing need huge amounts of stable RNAs in order to translate mRNAs into proteins [16, 61]. Conversely, cells in growth arrest have a limited translational activity and consequently no longer require high levels of stable RNAs. In the *E. coli* genome, the genes coding for these RNAs are organized in seven identical *rrn* operons, each of which is composed of the three genes for ribosomal RNA and one for transfer RNA [61, 99]. The expression of these RNAs is strongly stimulated by the Fis protein [99]. As production of stable RNAs is the hallmark of cellular growth, we will consider the cells to be committed to stationary phase when the *rrn* concentration is low.

How does the switch between growing or slowing down the growth emerge from the interconnections between the four network modules? The functioning of the individual modules can be understood intuitively to a certain extent. However, it is not known how the global behavior of the system emerges from the local interactions inside and between modules. A closer look at figure 2 reveals that it contains a number of positive and negative feedback loops that are suspected to play a fundamental role in controlling the growth transition. Examples of these feedback loops are the homeostatic control of DNA supercoiling and the cross-inhibition of *fis* and *crp*. The interactions making up these feedback loops are critical for the network connectivity, since they link the different modules together. In order to better understand the role of the feedback loops for the system dynamics, we have built a mathematical model of the regulatory network and simulated the behavior of the system.

To date no comprehensive mathematical models of the nutritional stress response network in figure 2 have been proposed, although some particularly well-studied parts of the network have been the subject of modeling studies. We mention, for example, the description of the DNA supercoiling level as

a function of the cellular energy charge [55, 104], the regulation of the transcription efficiency by the complex cAMP·CRP [66], as well as the carbohydrate uptake by the phosphotransferase system [30, 64, 93, 109]. However, the dynamics of the entire nutritional stress response network has never been studied, the principal reason being that, except for the above-mentioned network parts, quantitative data on kinetic parameters and molecular concentrations are not usually available. In order to deal with this lack of data, we use in this report a qualitative simulation method, described in the next section. This approach has allowed us to gain an understanding of how *E. coli* cells adapt their growth to different environmental conditions.

3 Qualitative simulation of genetic regulatory networks

The qualitative simulation method described in [24] is based on a class of piecewise-linear (PL) differential equation models that provide a coarse-grained description of genetic regulatory networks. The PL models have mathematical properties that allow qualitative predictions on the steady-state and transient behavior of the system to be made. Below, we give a brief summary of the method, focusing on the description of genetic regulatory networks by PL models and the predictions obtained from the models through qualitative simulation.

3.1 Piecewise-linear models of genetic regulatory networks

The dynamics of genetic regulatory networks can be modeled by a class of piecewise-linear (PL) differential equations originally proposed by Glass and Kauffman [34], and generalized by Mestl *et al.* [77]. The equations have the form

$$\dot{x}_i = f_i(\boldsymbol{x}) - g_i(\boldsymbol{x})\, x_i, \quad x_i \geq 0,\ 1 \leq i \leq n, \tag{1}$$

where $\boldsymbol{x} = (x_1, \ldots, x_n)'$ is a vector of cellular protein concentrations. The *state equations* (1) define the rate of change of the concentration x_i as the difference of the rate of synthesis $f_i(\boldsymbol{x})$ and the rate of degradation $g_i(\boldsymbol{x})\, x_i$ of the protein.

The function $f_i : \mathbb{R}^n_{\geq 0} \to \mathbb{R}_{\geq 0}$ expresses how the rate of synthesis of the protein encoded by gene i depends on the concentrations $\boldsymbol{x}$ of proteins in the cell. It is defined as

$$f_i(\boldsymbol{x}) = \sum_{l \in L} \kappa_{il}\, b_{il}(\boldsymbol{x}), \tag{2}$$

where κ_{il} is a rate parameter ($\kappa_{il} > 0$), $b_{il} : \mathbb{R}^n_{\geq 0} \to \{0, 1\}$ a *regulation function*, and L a possibly empty set of indices of regulation functions. The function g_i describes the regulation of protein degradation. It is defined analogously to f_i, except that we demand that $g_i(\boldsymbol{x})$ be strictly positive. In addition, in order to formally distinguish degradation rates from synthesis rates, we will denote the former by γ instead of κ. Notice that with the above definitions of f_i and g_i, the state equations (1) are *piecewise-linear (PL)*.

A regulation function b_{il} describes the logic of gene regulation [105]. More precisely, it describes the conditions under which the protein encoded by gene i is synthesized (degraded) at a rate κ_{il} ($\gamma_{il}\, x_i$). These conditions are formulated as expressions of step functions $s^+, s^- : \mathbb{R}^2 \to \{0, 1\}$:

$$s^+(x_j, \theta_j) = \begin{cases} 1, & x_j > \theta_j, \\ 0, & x_j < \theta_j, \end{cases} \qquad \text{and} \qquad s^-(x_j, \theta_j) = 1 - s^+(x_j, \theta_j), \tag{3}$$

where x_j is an element of the state vector $\boldsymbol{x}$, and θ_j a constant denoting a threshold concentration ($\theta_j > 0$). Notice that step functions $s^+(x_j, \theta_j)$ and $s^-(x_j, \theta_j)$ are not defined for $x_j = \theta_j$, so neither are the regulation functions in which they occur. We use regulation functions that are the arithmetic equivalent of logical functions, as described in [87].

The PL models can be extended to take into account *input variables* $\boldsymbol{u} = (u_1, \ldots, u_m)'$, representing the concentration of proteins and small molecules whose synthesis and degradation are regulated outside the system. This leads to models of the form:

$$\dot{x}_i = f_i(\boldsymbol{x}, \boldsymbol{u}) - g_i(\boldsymbol{x}, \boldsymbol{u})\, x_i, \quad x_i \geq 0,\ u_j \geq 0,\ 1 \leq i \leq n,\ 1 \leq j \leq m, \tag{4}$$

In what follows, we will assume that the input variables are constant, *i.e.*, $\dot{\boldsymbol{u}} = \boldsymbol{0}$. As a consequence, (4) can be reduced to (1) without loss of generality, by prior evaluation of the step-function expressions in which input variables occur.

3.2 Mathematical analysis of piecewise-linear models

The dynamical properties of the PL models can be analyzed in the n-dimensional phase space box $\Omega = \Omega_1 \times \ldots \times \Omega_n$, where every Ω_i, $1 \leq i \leq n$, is defined as

$$\Omega_i = \{x_i \in \mathbb{R}_{\geq 0} \mid 0 \leq x_i \leq max_i\}, \tag{5}$$

and max_i is a parameter denoting a maximum concentration for the protein.

Given that the protein encoded by gene i has p_i threshold concentrations, the $(n-1)$-dimensional threshold hyperplanes $x_i = \theta_i^{k_i}$, $1 \leq k_i \leq p_i$, partition Ω into hyperrectangular regions that are called *domains*. More precisely, a domain $D \subseteq \Omega$ is defined by $D = D_1 \times \ldots \times D_n$, where every D_i, $1 \leq i \leq n$, is given by one of the equations below:

$$\begin{aligned}
D_i =& \{x_i \mid 0 \leq x_i < \theta_i^1\},\\
D_i =& \{x_i \mid x_i = \theta_i^1\},\\
D_i =& \{x_i \mid \theta_i^1 < x_i < \theta_i^2\},\\
& \ldots\\
D_i =& \{x_i \mid \theta_i^{p_i} < x_i \leq max_i\}.
\end{aligned} \tag{6}$$

If for a domain D, there are some i, j, $1 \leq i \leq n$, $1 \leq j \leq p_i$, such that $D_i = \{x_i \mid x_i = \theta_i^j\}$, then D is called a *switching* domain. Otherwise, D is called a *regulatory domain*.

When evaluating the step-function expressions in (2) in a regulatory domain, $f_i(\boldsymbol{x})$ and $g_i(\boldsymbol{x})$ reduce to sums of rate constants. More precisely, in every regulatory domain $D \subseteq \Omega$, $f_i(\boldsymbol{x})$ reduces to some $\mu_i^D \in M_i \equiv \{f_i(\boldsymbol{x}) \mid \boldsymbol{0} \leq \boldsymbol{x} \leq \boldsymbol{max}\}$, and $g_i(\boldsymbol{x})$ to some $\nu_i^D \in N_i \equiv \{g_i(\boldsymbol{x}) \mid \boldsymbol{0} \leq \boldsymbol{x} \leq \boldsymbol{max}\}$. M_i and N_i collect the synthesis and degradation rates of the protein in different domains of Ω. It can be easily shown that all trajectories in D monotonically converge towards the so-called *target equilibrium*, lying at the intersection of the $(n-1)$-dimensional threshold hyperplanes $x_i = \mu_i^D/\nu_i^D$ $(1 \leq i \leq n)$ [34, 77, 105]. The target equilibrium level μ_i^D/ν_i^D of the protein concentration x_i gives an indication of the strength of gene expression in D. Call $\Psi(D) = \{(\mu_1^D/\nu_1^D, \ldots, \mu_n^D/\nu_n^D)'\}$ the *target equilibrium set* of D. If $\Psi(D) \cap D \neq \{\}$, then all solutions in D asymptotically approach the target equilibrium, which is then a stable equilibrium point of the system. If $\Psi(D) \cap D = \{\}$, the solutions will leave D at some point.

In switching domains, $f_i(\boldsymbol{x})$ and $g_i(\boldsymbol{x})$ are not defined in general, because some concentration variables assume a threshold value. Moreover, due to the use of step functions, $f_i(\boldsymbol{x})$ and $g_i(\boldsymbol{x})$ may be discontinuous at the $(n-k)$-dimensional threshold hyperplane in which the domain is contained $(1 \leq k \leq n)$. In order to cope with this problem, the system of differential equations (1) is extended into a system of differential inclusions, following an approach inspired by Filippov [24, 29, 39]. Using this generalization, it can be shown that, in the case of a switching domain D, the solution trajectories either cross D instantaneously or converge towards a target equilibrium set $\Psi(D)$ located in the threshold hyperplane containing D. Here, $\Psi(D)$ is the smallest hyperrectangle containing the target equilibria

of the regulatory domains that have D in their boundary, intersected with the threshold hyperplane containing D. In the case of switching domains, $\Psi(D)$ is generally not a single point. If $\Psi(D) \cap D = \{\}$ all solutions will leave D at some point. On the other hand, if $\Psi(D) \cap D \neq \{\}$, there exist solutions in D that reach or asympotically approach the target equilibrium set $\Psi(D)$ as $t \to \infty$. Every $\boldsymbol{\psi} \in \Psi(D) \cap D$ is an equilibrium point of the system. Whether this equilibrium point is stable or unstable must be determined through further analysis [18].

3.3 Qualitative description of dynamics of piecewise-linear models

The mathematical framework presented in the previous section suggests an intuitive qualitative description of the dynamics of regulatory systems described by PL models (1). This description is based on a discrete abstraction of the state of the system, a so-called *qualitative state*, consisting of the domain D in which the system resides and the position of the target equilibrium set $\Psi(D)$ with respect to D. A qualitative state thus captures the local dynamics of the system. There exists a *transition* between two qualitative states QS and QS', corresponding to contiguous domains D and D', if some solution trajectories starting in D reach D', without passing through an intermediate domain. The sets of qualitative states and transitions between qualitative states define a *state transition graph*, summarizing the qualitative dynamics of the regulatory system.

The state transition graph may contain one or more *qualitative equilibrium states*, each of which corresponds to an equilibrium point of the system. A path in the state transition graph is called a *qualitative behavior*. It describes how the bounds on protein concentrations evolve over time, according to the sequence of transitions between qualitative states. A cyclic qualitative behavior, a so-called *qualitative cycle*, may correspond to a limit cycle or to trajectories spiraling towards or from an equilibrium point. The set of qualitative states from which a qualitative equilibrium state or qualitative cycle is reachable form its *attraction set*. The qualitative nature of the state transition graph is well-adapted to measurement techniques in genomics, which currently have limited quantitative precision, but are able to detect qualitative changes in gene expression over time.

3.4 Qualitative piecewise-linear models

Most of the time, precise numerical values for the threshold and rate parameters in a PL model are not available. However, instead of specifying precise numerical values, it is often possible to supplement the state equations with inequality constraints on the parameter values. The inequality constraints express weak, but reliable information about the regulatory interactions that can be inferred from biological data. The resulting, so-called *qualitative PL model*, subsumes a set of quantitative PL models, the qualitative dynamics of each of which can be described by means of a state transition graph.

The first type of constraint, the *threshold inequalities*, are obtained by ordering the p_i threshold concentrations of the protein encoded by gene i, *i.e.*,

$$0 < \theta_i^1 < \ldots < \theta_i^{p_i} < max_i. \tag{7}$$

The threshold inequalities determine the partitioning of Ω into regulatory and switching domains.

The second type of constraint, the *equilibrium inequalities*, order the possible target equilibrium levels of x_i in different regulatory domains D with respect to the threshold concentrations. Biologically speaking, the equilibrium inequalities define the strength of gene expression in the domain in a qualitative way, on the scale of ordered threshold concentrations. More precisely, for every $\mu_i \in M_i$, $\nu_i \in N_i$, and $\mu_i, \nu_i \neq 0$, we specify one of the following pairs of inequalities:

$$
\begin{aligned}
&0 < \mu_i/\nu_i < \theta_i^1, \\
&\theta_i^1 < \mu_i/\nu_i < \theta_i^2, \\
&\ldots \\
&\theta_i^{p_i} < \mu_i/\nu_i < max_i.
\end{aligned} \tag{8}
$$

The equilibrium inequalities constrain the relative position of D and its target equilibrium set $\Psi(D)$.

The models of genetic regulatory networks treated by the simulation method consist of state equations (1), supplemented by parameter inequalities (7) and (8). Every such *qualitative* PL model corresponds to a set of *quantitative* PL models consisting of state equations (1) and a particular combination of numerical parameter values consistent with the parameter inequalities. It has been shown that in the region of the parameter space defined by the inequalities in the qualitative PL model, all quantitative PL models yield the same state transition graph [24]. This graph can be efficiently computed from the inequality constraints by symbolic instead of numerical means.

3.5 Qualitative simulation

A state transition graph may become exceedingly large, as the number of domains, and hence qualitative states, grows exponentially with the dimension of the system. For many purposes, it is sufficient to know which qualitative states are reachable from a given initial qualitative state, that is, which qualitative behaviors the system can exhibit when initially being in this state. The algorithm for *qualitative simulation* described in [24] generates the reachable part of a state transition graph from a qualitative PL model and an initial domain.

The state transition graph generated through qualitative simulation is a prediction of the qualitative dynamics of the system. We have demonstrated that this state transition graph covers all qualitative behaviors permitted by any one of the quantitative PL models subsumed by the qualitative PL models [24]. That is, whatever the exact numerical values for the parameters may be, if these values are consistent with the threshold and equilibrium inequalities specified in the qualitative PL model, the qualitative shape of the solution is described by a sequence of states in the state transition graph. The inverse is not true: the state transition graph resulting from a qualitative simulation may contain qualitative behaviors that are not permitted by some quantitative PL model subsumed by the qualitative PL model.

The simulation method has been implemented in Java 1.4, in a program called *GNA (Genetic Network Analyzer)* [23].[1] In order to facilitate its use, the program is equipped with a graphical user interface, called *VisualGNA*. The interface includes a model editor, which integrates the specification of models of genetic regulatory networks with the simulation of the behavior of the network and the biological interpretation of the simulation results. The model editor structures and facilitates the specification of the differential equations and inequality constraints by means of check boxes, item lists, formatted text fields, and completion keys. In addition, it performs syntactic and semantic checks to guarantee the consistency and completeness of information entered by the user. VisualGNA also supports the visual analysis of state transition graphs by allowing the user, among other things, to zoom in on or zoom out from state transition graphs, to reduce or expand state transition graphs, and to highlight qualitative states in the graph that satisfy certain user-specified specific criteria. In order to analyze large and complex state transition graphs in more detail, GNA allows the simulation results to be exported to standard model-checking tools [13]. Figure 3 contains a screenshot of GNA, showing the results of a qualitative simulation of the *E. coli* stress response network (section 6).

[1] GNA is available for non-profit academic research purposes at `http://www-helix.inrialpes.fr/gna`.

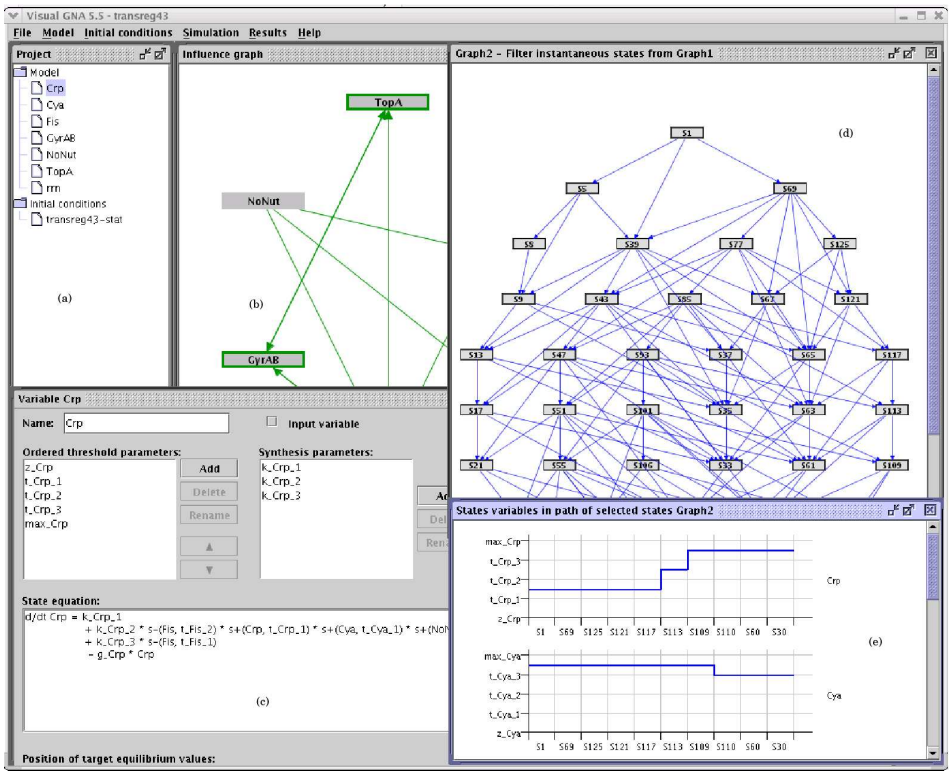

Figure 3: Screenshot of the graphical user interface VisualGNA of the qualitative simulator GNA: (a) Tree of model variables and initial conditions, (b) interaction graph, (c) specification of equations and inequalities for a variable, (d) state transition graph, and (e) qualitative temporal evolution of some model variables.

4 Modeling of interactions in the nutritional stress response network

In this section, we describe how the different types of interaction that play a role in the nutritional stress response can be modeled by means of piecewise-linear differential equations using step functions. More particularly, we cover the cases where gene expression is controlled by a transcriptional regulator (section 4.1), by a transcriptional regulator modified through a signal-transduction pathway (section 4.2) and by DNA topology (section 4.3). The resulting model components are combined in the following section, where a state equation for each of the proteins or RNAs in the nutritional stress response network is given.

4.1 Transcriptional regulator

The control of the expression of stable RNAs by the global regulator Fis is an example of gene-expression regulation by a transcriptional activator. During exponential phase, when the demand for protein synthesis is high, promoters of the seven *rrn* operons account for more than 60% of the cellular transcription products [16]. The high activity of these promoters has been correlated with their stimulation by the protein Fis [8, 82, 122, 123]. In particular, the protein activates transcription by binding to regulatory sites and stabilizing the interaction between RNA polymerase and ribosomal promoters in a cooperative manner [5, 72, 49, 99, 124]. The regulatory mechanism, shown in figure 4(a), can be modeled by means of a sigmoidal function, the Hill rate law (Appendix A.1). Figure 5(a) shows the activity of the *rrn* promoter, and hence the rate of synthesis of stable RNAs, as a function of the cellular concentration x_{fis} of Fis. Below a certain threshold concentration of Fis, the stable RNA genes will be poorly expressed, whereas above this threshold their expression will reach its maximum level.

(a) (b)

Figure 4: Regulation of the expression of (a) *rrn* and (b) *fis* by the protein Fis.

The sigmoid curve in figure 5(a) can be approximated by a step function. The rate of expression of stable RNAs can thus be expressed in the following manner:

$$f_{rrn}(x_{fis}) = \kappa_{rrn}\ s^{+}(x_{fis}, \theta^{3}_{fis}), \tag{9}$$

where κ_{rrn} and θ^{3}_{fis} are constants denoting the synthesis rate of stable RNAs and the threshold concentration of Fis, respectively. The function $f_{rrn}(x_{fis})$ states that stable RNAs are expressed at a rate κ_{rrn}, if $x_{fis} > \theta^{3}_{fis}$, whereas they are not expressed if $x_{fis} < \theta^{3}_{fis}$.

In addition to activating *rrn* production, Fis has been shown to repress its own expression, by binding to the promoter region of the gene [10, 83, 89]. As in the previous example, the activity plot of *fis* is a sigmoidal curve (figure 5(b)). However, expression of this gene is now a decreasing function of the Fis concentration. Moreover, the curve is shifted to a higher concentration range, which reflects the fact that Fis binds more weakly to its own promoter region than to the one of *rrn*. The curve in figure 5(b) can be approximated by the following step function:

$$f_{fis}(x_{fis}) = \kappa_{fis}\ s^{-}(x_{fis}, \theta^{5}_{fis}), \tag{10}$$

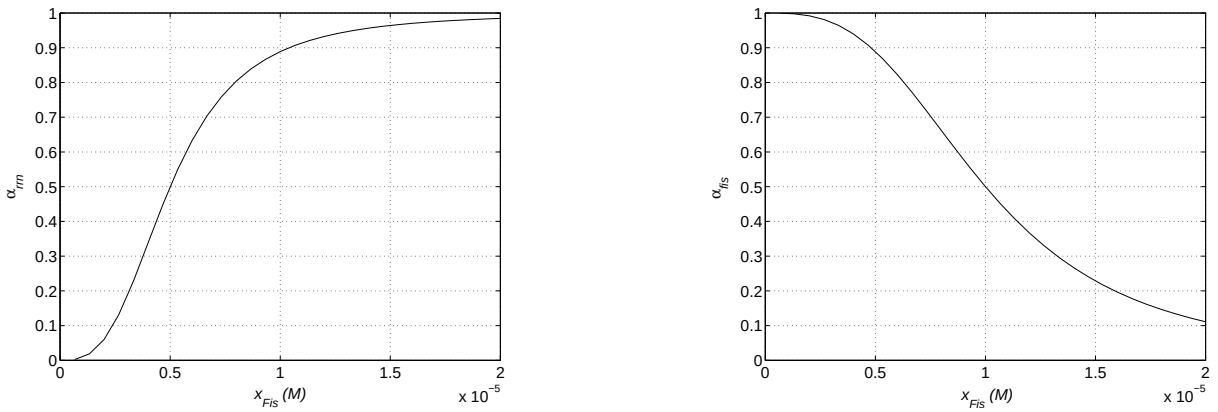

(a) (b)

Figure 5: (a) Activity of the promoter *rrn* P1 (α_{rrn}), normalized on the scale 0 to 1, as a function of the concentration of the transcriptional regulator Fis (x_{fis}). (b) Idem for the activity of the promoter *fis* P (α_{fis}). The activity plots have been generated from the model and parameters values in Appendix A.1.

where κ_{fis} is a synthesis rate, θ^5_{fis} a threshold concentration, and $\theta^5_{fis} > \theta^3_{fis}$.

In reality, the regulation of the expression of *rrn* and *fis* presented in Fig. 5 is even more complex: transcription of the gene *fis* is also controlled by the cAMP·CRP complex, while the synthesis of stable RNAs occurs from two instead of one promoter. This added complexity has been omitted for the purpose of the above examples, but will be fully described in section 5.

4.2 Transcriptional regulator activated through a signal-transduction pathway

As seen previously in section 2, the CRP global regulator is activated through a signal-transduction pathway, in response to a lack of nutrients. More precisely, CRP forms a complex with cAMP, as soon as this metabolite is synthesized from ATP by the active form of adenylate cyclase Cya [37, 42, 97]. The cAMP·CRP complex is able to regulate the expression of a large number of genes. It interacts with specific sequences in cAMP·CRP-responsive promoters, and either promotes transcriptional initiation by stabilizing RNA polymerase, or represses initiation of transcription mostly through competitive binding to the promoter [17, 68, 97]. The cAMP·CRP complex is also able to control its own production by activating transcription of the gene *crp* [41, 53] or repressing transcription of the gene *cya* [3, 4, 11, 51, 60, 78]. The corresponding regulatory mechanisms are presented in figure 6.

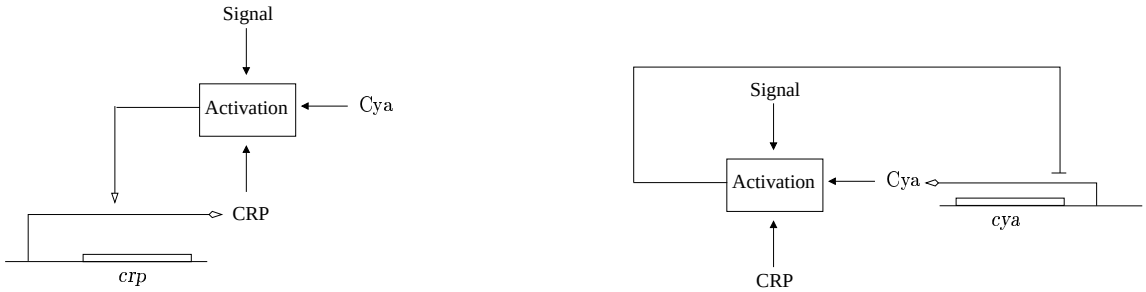

(a) (b)

Figure 6: Regulation of the expression of (a) *crp* and (b) *cya* by the active complex cAMP·CRP.

Based on the extensive literature concerning cAMP·CRP, we have been able to establish a detailed kinetic model for the above regulatory mechanism, using the mass-action law and the Hill rate law (appendix A.2, see also [66] for an example of a CRP regulation model). Because the synthesis of cAMP as well as its association or dissociation with CRP takes place on a much faster time-scale than the synthesis and degradation of proteins, we can assume that these former processes are in quasi-equilibrium with respect to the latter. This gives rise to a steady-state model that can be used to calculate the activity of the *crp* promoter as a function of the total CRP and Cya concentrations (x_{crp} and x_{cya}), in the absence and presence of Signal. The gene activity plot in figure 7(a) shows that, if Signal is absent, *crp* is never expressed. Yet, if Signal is present, we obtain the sigmoidal surface plotted in figure 7(b).

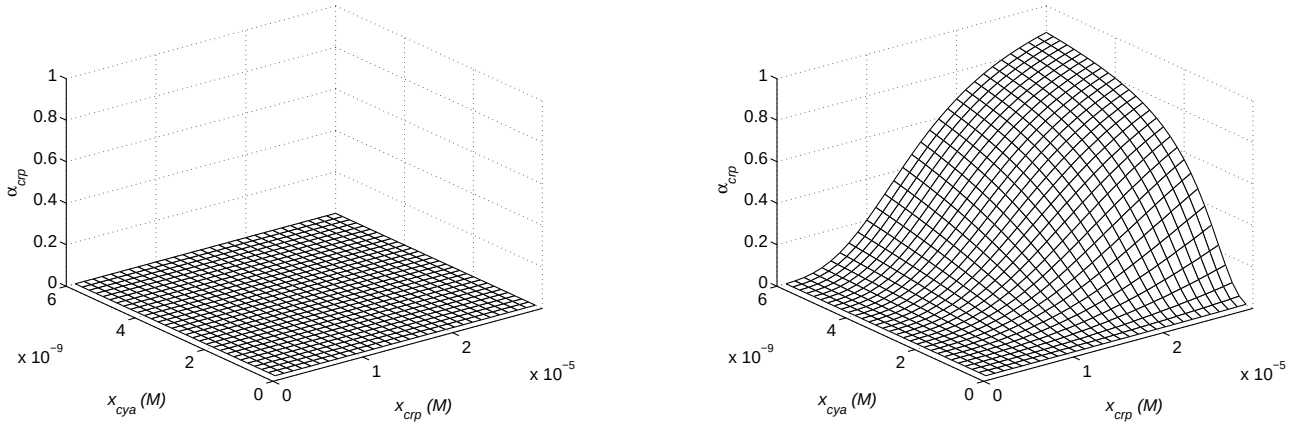

Figure 7: Activity of the gene *crp* (α_{crp}), normalized on the scale 0 to 1, as a function of the total concentration of CRP (x_{crp}) and Cya (x_{crp}), in absence of Signal (a) and in its presence (b). The activity plots have been generated from the model and parameters values in Appendix A.2.

Let the input variable u_s denote the nutritional stress signal. The step function $s^+(u_s, \theta_s)$ evaluates to 1 if Signal is present, and to 0, if it is absent. Then the plots in figure 7 give rise to the following step-function approximation for the synthesis rate of *crp*:

$$f_{crp}(x_{crp}, x_{cya}, u_s) = \kappa^2_{crp}\ s^+(x_{crp}, \theta^1_{crp})\ s^+(x_{cya}, \theta^1_{cya})\ s^+(u_s, \theta_s). \tag{11}$$

κ^2_{crp} is a rate parameter, while θ^1_{crp} and θ^1_{cya} are threshold parameters for x_{crp} and x_{cya}, respectively. The function $f_{crp}(x_{crp}, x_{cya}, u_s)$ formalizes the regulatory logic shown in the plots. In particular, if the nutritional stress signal is present ($s^+(u_s, \theta_s) = 1$), then gene *crp* is expressed at a rate κ^2_{crp}, if and only if $x_{crp} > \theta^1_{crp}$ and $x_{cya} > \theta^1_{cya}$. If the nutritional stress signal is absent, then *crp* is not expressed.

At a higher concentration, the cAMP·CRP complex inhibits *cya* expression (figure 6(b)) [3, 4, 51, 60, 78]. Repeating the above analysis results in the *cya* activity plots presented in figure 8. The sigmoidal curve in figure 8(b) is inversed due to the repressive effect of cAMP·CRP on *cya* expression. Moreover, it is shifted to a different region of the concentration space, because a high level of the cAMP·CRP complex is required to repress the *cya* promoter [97]. The regulatory logic of *cya* is approximated by

$$f_{cya}(x_{crp}, x_{cya}, u_s) = \kappa^2_{cya}\ (1 - s^+(x_{crp}, \theta^3_{crp})\ s^+(x_{cya}, \theta^3_{cya})\ s^+(u_s, \theta_s)), \tag{12}$$

with $\theta^1_{crp} < \theta^3_{crp}$ and $\theta^1_{cya} < \theta^3_{cya}$.

The step-function expressions (11)-(12) describe only part of the regulatory logic of the genes *crp* and *cya*. A complete description of the control of expression of these genes will be given in section 5.

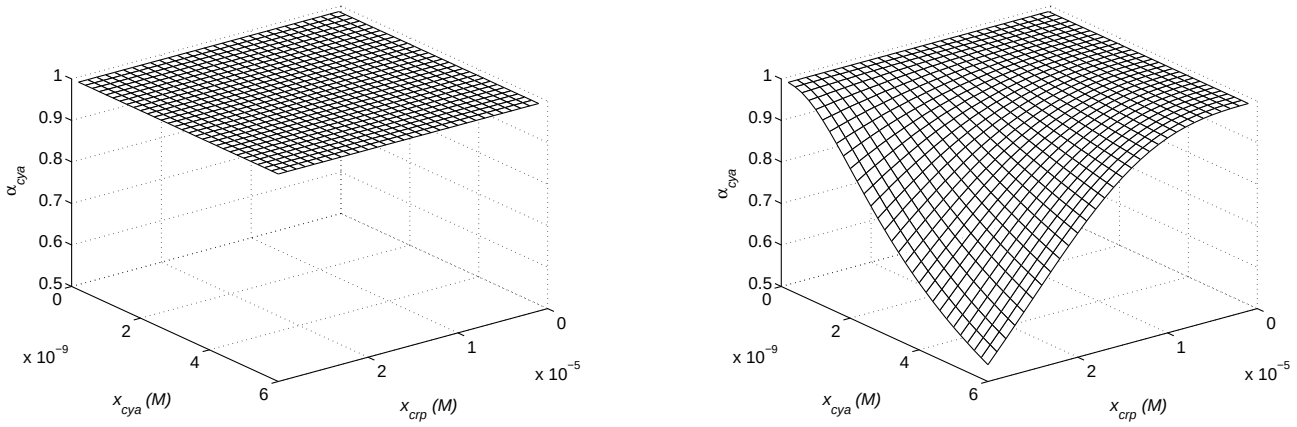

(a) (b)

Figure 8: Activity of the gene *cya* (α_{cya}), normalized on the scale 0 to 1, as a function of the total concentration of CRP (x_{crp}) and Cya (x_{crp}), in absence of Signal (a) and in its presence (b). The activity plots have been generated from the model and parameters values in Appendix A.2.

4.3 DNA supercoiling

DNA supercoiling constrains the topological structure of DNA, and thus influences gene expression through a complicated mechanism. DNA topology is controlled by two enzymes, GyrAB and TopA, but responds to other physical and chemical parameters factors as well [25, 44, 92]. Depending on the relative concentration of the two enzymes, DNA supercoiling can reach different levels in the cell: in the presence of high amounts of GyrAB, many negative supercoils are introduced into the DNA, whereas these are relaxed when the TopA concentration is high. The supercoiling level controls the expression of the *topA* and *gyrAB* genes, as shown in figure 9.

(a) (b)

Figure 9: Regulation of the expression of (a) *fis* and (b) *gyrAB* by the DNA supercoiling level.

The mechanism of the control of gene expression by DNA supercoiling is particularly difficult to model because the action of the two bacterial topoisomerases occurs through *chemical* reactions that produce a *physical* effect, a change in the helical twist of DNA [44]. Existing mathematical models of DNA supercoiling have only studied each aspect of this phenomenon in isolation, adopting either a biophysical or a biochemical point of view. On the one hand, they have described, for example, the local melting of torsionally-stressed DNA [15] or the elastic deformation of DNA [14, 120]. On the

other hand, metabolic control analysis has been applied to the homeostatic control of DNA supercoiling by GyrAB and TopA [55, 104]. In order to integrate the physical and biochemical points of view, we have derived an empirical model that is consistent with available data on GyrAB and TopA action and transcription regulation by DNA topology. The model takes into account the fact that the ratio of the GyrAB and TopA concentrations determines the DNA supercoiling level, and that the supercoiling level stimulates the initiation of transcription by RNA polymerase, through a sigmoidal response curve mediated by its capacity to locally unwind DNA in the promoter region [44] (Appendix A.3). This enables us to calculate the *fis* promoter activity as a function of the GyrAB and TopA concentrations, as shown in the activity plot in figure 10(a). The plot expresses the competition between the two topoisomerases: the activity of *fis* increases with increasing concentrations of GyrAB and decreasing concentrations of TopA, in agreement with reported data [101].

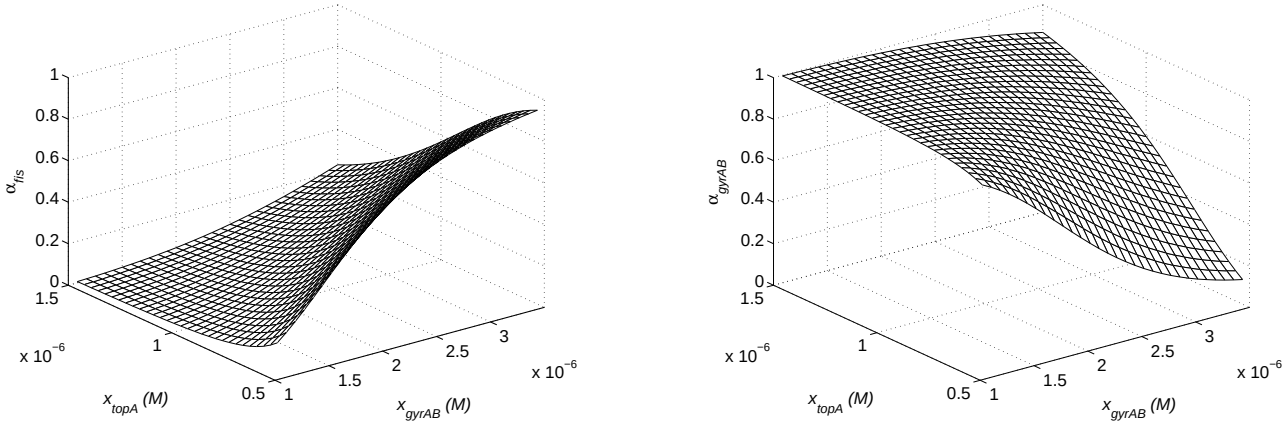

(a) (b)

Figure 10: (a) Activity of the promoter *fis* P (α_{fis}), normalized on the scale 0 to 1, as a function of the concentration of TopA (x_{topA}) and GyrAB (x_{gyrAB}). (b) Idem for the activity of the promoter *gyrAB* P (α_{gyrAB}). The activity plots have been generated from the model and parameters values in Appendix A.3.

Similar to the approach followed for the cAMP·CRP example, the sigmoidal surface can be approximated by means of step functions, yielding the following expression for the rate of synthesis from the *fis* promoter:

$$f_{fis}(x_{gyrAB}, x_{topA}) = \kappa^2_{fis}\ s^+(x_{gyrAB}, \theta^2_{gyrAB})\ s^-(x_{topA}, \theta^2_{topA}), \tag{13}$$

where κ^2_{fis} is a synthesis rate, and θ^2_{gyrAB}, θ^2_{topA} are threshold concentrations of GyrAB and TopA, respectively. The function $f_{fis}(x_{gyrAB}, x_{topA})$ states that Fis is expressed at a rate κ_{fis}, if $x_{gyrAB} > \theta^2_{gyrAB}$ and $x_{topA} < \theta^2_{topA}$. If this condition is not satisfied, the gene is not expressed.

When DNA supercoiling level has reached a higher level, it is able to regulate other genes, such as *gyrAB* (figure 9(b)) [74, 76, 104]. Using the above-mentioned empirical model to determine the activity plots, we obtain an inverse sigmoidal surface, due to the fact that DNA supercoiling decreases *gyrAB* expression (figure 10(b)). In addition, the surface is shifted to a different region of the concentration space, reflecting the higher level at which DNA supercoiling regulates *gyrAB*. The approximation of the activity plot using step functions now becomes:

$$f_{gyrAB}(x_{gyrAB}, x_{topA}) = \kappa^2_{gyrAB}\ (1 - s^+(x_{gyrAB}, \theta^3_{gyrAB})\ s^-(x_{topA}, \theta^1_{topA})), \tag{14}$$

with $\theta^3_{gyrAB} > \theta^2_{gyrAB}$ and $\theta^1_{topA} < \theta^2_{topA}$.

In reality, the regulation of *fis* and *gyrAB* is more complex than suggested by the above examples (see figure 2). A complete description of the control of these genes will be given in section 5.

5 Modeling of the nutritional stress response network

In order to model the nutritional stress network of figure 2, we will define the state equations and parameters inequalities for the genes involved in each of the four modules: the input module (section 5.1), the CRP activation module (section 5.2), the DNA topology module (section 5.3) and the output module (section 5.4). The equations and inequalities making up the model are summarized in figure 11.

5.1 Input module

A signal-transduction pathway involving the PTS system is responsible for transmitting the information of a lack of nutrient to the processes taking place inside an *E. coli* cell [88]. In particular, it drives activation of the adenylate cyclase, Cya, responsible for the synthesis of cAMP. As explained in section 2, we simplify the signal-transduction pathway, for which detailed kinetic models exist [30, 65, 93, 109, 115] to a nutritional stress signal that directly activates Cya. It is associated with the input variable u_s, which is considered to be constant, that is,

$$\dot{u}_s = 0. \tag{15}$$

We define a single threshold for Signal, θ_s, giving the following inequalities:

$$0 < \theta_s < max_s. \tag{16}$$

If the step function $s^+(u_s, \theta_s)$ evaluates to 1(0), then Signal is said to be present (absent). The presence of Signal denotes conditions of nutrient deprivation that mark the entry into stationary phase.

5.2 CRP activation module

The CRP activation module is composed of the proteins Cya, CRP, and Fis. When activated by Signal, Cya produces the metabolite cAMP, that binds CRP and thus enables it to regulate gene expression [42, 88, 97].

Gene *crp* is expressed from two promoters, P1 and P2 [2, 36]. Their regulation accounts for the control of expression of the CRP protein, in response to the availability of carbon compounds such as glucose [53, 54, 97]. The protein Fis inhibits both promoters [36], whereas the complex cAMP·CRP controls only promoter P1, through a regulatory mechanism that is still unclear. The available data show that the complex is able to both repress and activate *crp* P1 by binding to regulatory sites around the promoter [2, 40, 41, 53, 84, 85]. However, in order to simplify, we omit the negative control of *crp* P1, because this mechanism plays a role only during the exponential growth phase, when the concentration of CRP is low [53].[2] We denote by κ^1_{crp} the background synthesis rate from promoter P1 during exponential growth, by κ^2_{crp} the synthesis rate induced by derepression of this promoter, and by κ^3_{crp} the synthesis rate from promoter P2. With a degradation rate equal to $\gamma_{crp}\ x_{crp}$, we obtain the following state equation for x_{crp}:

$$\dot{x}_{crp} = \kappa^1_{crp} + \kappa^2_{crp}\ s^-(x_{fis}, \theta^2_{fis})\ s^+(x_{crp}, \theta^1_{crp})\ s^+(x_{cya}, \theta^1_{cya})\ s^+(u_s, \theta_s) + \kappa^3_{crp} s^-(x_{fis}, \theta^1_{fis}) - \gamma_{crp}\ x_{crp}. \tag{17}$$

[2] We also developed a more complex model involving the negative control of *crp* P1 by cAMP·CRP, but we found that the added complexity does not have any effect on the conclusions of this study.

The thresholds in the step-function expressions for Fis-mediated repression ($s^-(x_{fis}, \theta^1_{fis})$ and $s^-(x_{fis}, \theta^2_{fis})$) reflect the fact that Fis binds preferentially to the *crp* P2 promoter region, rather than to the *crp* P1 promoter region [36].

Different concentration thresholds of CRP are required in the cells, to allow production of different levels of the cAMP·CRP complex. Indeed, a low concentration of the complex is sufficient to stimulate *crp* expression in the presence of the nutritional-stress signal. Above a second, higher threshold concentration, the complex controls the expression of a large set of genes involved in the adaptation of *E. coli* cells to the entry into stationary phase. Finally, above its highest threshold concentration, the complex inhibits its further accumulation, by shutting off its production through repression of *cya*. This leads to three threshold concentrations of CRP, denoted by θ^1_{crp}, θ^2_{crp} and θ^3_{crp}, which are ordered by the threshold inequalities

$$0 < \theta^1_{crp} < \theta^2_{crp} < \theta^3_{crp} < max_{crp}. \tag{18}$$

By means of (17), we derive the possible synthesis and degradation rates of CRP, $M_{crp} = \{\kappa^1_{crp}, \kappa^1_{crp} + \kappa^2_{crp}, \kappa^1_{crp} + \kappa^3_{crp}, \kappa^1_{crp} + \kappa^2_{crp} + \kappa^3_{crp}\}$ and $N_{crp} = \{\gamma_{crp}\}$, respectively. Because *crp* P1 is a house-keeping promoter [36], we set $\kappa^1_{crp}/\gamma_{crp} > \theta^1_{crp}$ and $(\kappa^1_{crp} + \kappa^2_{crp})/\gamma_{crp} > \theta^1_{crp}$. If this were not the case, CRP would not be able to reach a basal concentration at which it can stimulate its own expression when Signal is switched on. The fact that *crp* P2 is a strong promoter [36] implies that $(\kappa^1_{crp} + \kappa^3_{crp})/\gamma_{crp} > \theta^3_{crp}$ and $(\kappa^1_{crp} + \kappa^2_{crp} + \kappa^3_{crp})/\gamma_{crp} > \theta^3_{crp}$, because this allows CRP to reach a level at which regulation of *cya* occurs. We thus arrive at the following equilibrium inequalities

$$\begin{aligned} \theta^1_{crp} < \frac{\kappa^1_{crp}}{\gamma_{crp}} < \theta^2_{crp}, \quad \theta^1_{crp} < \frac{\kappa^1_{crp} + \kappa^2_{crp}}{\gamma_{crp}} < \theta^2_{crp}, \\ \theta^3_{crp} < \frac{\kappa^1_{crp} + \kappa^3_{crp}}{\gamma_{crp}} < max_{crp}, \quad \theta^3_{crp} < \frac{\kappa^1_{crp} + \kappa^2_{crp} + \kappa^3_{crp}}{\gamma_{crp}} < max_{crp}. \end{aligned} \tag{19}$$

Cya is present at low concentrations in the cell [119]. It is the product of the gene *cya*, which is transcribed from three promoters: the constitutive P1 and P'1 promoters, and the regulated P2 promoter [3, 4, 96, 95]. Control of expression of *cya* is regulated by the complex cAMP·CRP, which represses gene transcription starting from the strong promoter P2 [3, 4, 51, 60, 78]. We use the rate constants κ^1_{cya} and κ^2_{cya} to denote constitutive and cAMP·CRP-controlled synthesis of Cya.[3] In the absence of information to the contrary, degradation of Cya is assumed to occur spontaneously, with a rate constant γ_{cya}. Denoting by x_{cya} the total concentration of Cya, we arrive at the following state equation:

$$\dot{x}_{cya} = \kappa^1_{cya} + \kappa^2_{cya}\ (1 - s^+(x_{crp}, \theta^3_{crp})\ s^+(x_{cya}, \theta^3_{cya})\ s^+(u_s, \theta_s)) - \gamma_{cya}\ x_{cya}. \tag{20}$$

Because the complex cAMP·CRP exerts its regulatory functions at different thresholds in our model, following the reasoning of section 4.2, we define the same number of thresholds for x_{cya} as for x_{crp}. We thus obtain the three thresholds θ^1_{cya}, θ^2_{cya}, θ^3_{cya} with the following inequalities:

$$0 < \theta^1_{cya} < \theta^2_{cya} < \theta^3_{cya} < max_{cya}. \tag{21}$$

The possible synthesis and degradation rates of Cya can be deduced from (20). They are $M_{cya} = \{\kappa^1_{cya}, \kappa^1_{cya} + \kappa^2_{cya}\}$ and $N_{cya} = \{\gamma_{cya}\}$, respectively. P1 and P'1 are house-keeping promoters, allowing a constitutive expression of Cya during *E. coli*'s life cycle and hence $\kappa^1_{cya}/\gamma_{cya} > \theta^1_{cya}$. Derepression

[3] Several reports indicate that Cya activity is also indirectly regulated by the cAMP·CRP complex, through the control of the activity of a PTS component, $EIIA^{Glc}$ [51, 56, 67, 107]. Because the exact mechanisms involved have not been elucidated so far, we omit this level of regulation.

of promoter P2 allows, together with P1, maximal production of Cya. As a consequence, $(\kappa^1_{cya} + \kappa^2_{cya})/\gamma_{cya} > \theta^3_{cya}$. In summary, we have the following equilibrium inequalities

$$\theta^1_{cya} < \frac{\kappa^1_{cya}}{\gamma_{cya}} < \theta^2_{cya}, \quad \theta^3_{cya} < \frac{\kappa^1_{cya} + \kappa^2_{cya}}{\gamma_{cya}} < max_{cya}. \tag{22}$$

The protein Fis is highly expressed at the beginning of exponential phase, during which it controls the expression of genes involved in metabolism. The protein is no longer detectable at the onset of stationary phase [6, 10, 89]. The expression of Fis is controlled at the transcriptional level, where it is produced from a unique promoter [70, 83, 114], instead of four promoters, as previously suggested [81]. The central position of Fis in the nutritional stress response network is reflected by the fact that the transcription of its gene is regulated by the cAMP·CRP complex, DNA supercoiling, as well as by Fis itself. We distinguish two physiologically-relevant synthesis rates for Fis, κ^1_{fis} and κ^2_{fis}, depending on whether the DNA supercoiling level regulates expression of Fis. The protein is degraded at a rate $\gamma_{fis}\ x_{fis}$ [6, 10, 82, 89]. Denoting by x_{fis} the total concentration of Fis, we arrive at the following state equation for the protein

$$\begin{aligned}\dot{x}_{fis} = \kappa^1_{fis}\ (1 - s^+(x_{crp}, \theta^1_{crp})\ s^+(x_{cya}, \theta^1_{cya})\ s^+(u_s, \theta_s))s^-(x_{fis}, \theta^5_{fis}) + \kappa^2_{fis}\ s^+(x_{gyrAB}, \theta^2_{gyrAB}) \\ \cdot\ s^-(x_{topA}, \theta^2_{topA})s^-(x_{fis}, \theta^5_{fis})\ (1 - s^+(x_{crp}, \theta^1_{crp})\ s^+(x_{cya}, \theta^1_{cya})\ s^+(u_s, \theta_s)) - \gamma_{fis}x_{fis}.\end{aligned} \tag{23}$$

Fis has five threshold concentrations, θ^1_{fis}, ..., θ^5_{fis}. The first two of these correspond to concentration levels above which Fis represses the two *crp* promoters. θ^3_{fis} corresponds to stimulation of *rrn* production. Control of *gyrAB* and *topA* promoters is exerted above the threshold θ^4_{fis}, whereas the protein represses its own expression above the threshold θ^5_{fis}. These five thresholds are ordered by the following inequalities

$$0 < \theta^1_{fis} < \theta^2_{fis} < \theta^3_{fis} < \theta^4_{fis} < \theta^5_{fis} < max_{fis}. \tag{24}$$

The possible synthesis and degradation rates are given by $M_{fis} = \{\kappa^1_{fis}, \kappa^1_{fis} + \kappa^2_{fis}\}$ and $N_{fis} = \{\gamma_{fis}\}$, respectively. We have to order the target equilibrium values $\kappa^1_{fis}/\gamma_{fis}$ and $\kappa^1_{fis} + \kappa^2_{fis}/\gamma_{fis}$ with respect to the threshold values. During exponential phase, Fis concentration should always be high enough to repress the strong promoter *crp* P2, in order to maintain CRP concentration at a low level, which gives $\kappa^1_{fis}/\gamma_{fis} > \theta^1_{fis}$. Making the reasonable assumption that the Fis concentration may reach a level at which the negative feedback loop becomes active (23) implies $\kappa^1_{fis} + \kappa^2_{fis} > \theta^5_{fis}$. We thus have the following equilibrium inequalities for Fis:

$$\theta^1_{fis} < \frac{\kappa^1_{fis}}{\gamma_{fis}} < \theta^2_{fis}, \quad \theta^5_{fis} < \frac{\kappa^1_{fis} + \kappa^2_{fis}}{\gamma_{fis}} < max_{fis}. \tag{25}$$

5.3 DNA topology module

The DNA topology module contains genes encoding GyrAB, TopA, and Fis. These three proteins are involved in the homeostatic control of DNA topology in *E. coli* cells [55, 74, 101, 104, 111]. They ensure a fine-tuned control of the DNA supercoiling level, except during growth transitions, when DNA topology changes, for example as glucose becomes depleted in the growth medium [9].

As explained in section 2, we consider the GyrAB complex as the product of a single gene *gyrAB*. This gene is transcribed from a unique promoter, whose activity is regulated by DNA supercoiling and the protein Fis [1, 74, 75, 76]. We consider two synthesis rates for the GyrAB complex: κ^1_{gyrAB} denotes the background expression of GyrAB and κ^2_{gyrAB} the synthesis rate induced by derepression of the promoter. The protein is degraded at a rate $\gamma_{gyrAB}x_{gyrAB}$. We thus obtain the following state equation for GyrAB:

$$\dot{x}_{gyrAB} = \kappa^1_{gyrAB} + \kappa^2_{gyrAB}\ (1 - s^+(x_{gyrAB}, \theta^3_{gyrAB})\ s^-(x_{topA}, \theta^1_{topA}))\ s^-(x_{fis}, \theta^4_{fis}) - \gamma_{gyrAB}x_{gyrAB}. \tag{26}$$

The possible synthesis and degradation rates can be deduced from equation (26): $M_{gyrAB} = \{\kappa^1_{gyrAB}, \kappa^1_{gyrAB} + \kappa^2_{gyrAB}\}$ and $N_{gyrAB} = \{\gamma_{gyrAB}\}$. Because there are three different thresholds at which the DNA supercoiling level controls gene expression, we should consider three different thresholds for GyrAB, θ^1_{gyrAB}, θ^2_{gyrAB} and θ^3_{gyrAB} (see section 4.3). They are ordered by means of the following inequalities:

$$0 < \theta^1_{gyrAB} < \theta^2_{gyrAB} < \theta^3_{gyrAB} < max_{gyrAB}. \tag{27}$$

In order to allow DNA topology to attain the level at which autoregulation sets in, GyrAB should reach its maximal concentration threshold, that is, $(\kappa^1_{gyrAB} + \kappa^2_{gyrAB})/\gamma_{gyrAB} > \theta^3_{gyrAB}$. An increase of Fis concentration and DNA supercoiling level shuts off transcription from the *gyrAB* promoter, which yields the constraint $\kappa^1_{gyrAB}/\gamma_{gyrAB} < \theta^1_{gyrAB}$. We thus obtain the following equilibrium inequalities:

$$0 < \frac{\kappa^1_{gyrAB}}{\gamma_{gyrAB}} < \theta^1_{gyrAB}, \quad \theta^3_{gyrAB} < \frac{\kappa^1_{gyrAB} + \kappa^2_{gyrAB}}{\gamma_{gyrAB}} < max_{gyrAB}. \tag{28}$$

The gene *topA* is transcribed from five promoters, whose exact contribution to the TopA expression level is not yet well-understood [91, 112]. They most likely allow expression of the topoisomerase under a wide range of environmental conditions. For the sake of simplicity, we consider *topA* here as being expressed from a single promoter. The expression of this gene is also controlled by Fis and DNA supercoiling, but in comparison with *gyrAB* in the opposite way: *topA* is activated by a low level of DNA supercoiling and by Fis [111, 116]. We distinguish two different synthesis rates for TopA: κ^1_{topA} represents TopA background expression and κ^2_{topA} corresponds to the additional synthesis rate when the *topA* promoter is activated by DNA topology and by Fis. With a degradation rate equal to $\gamma_{topA}\ x_{topA}$, we arrive at the following state equation

$$\dot{x}_{topA} = \kappa^1_{topA} + \kappa^2_{topA}\ s^+(x_{gyrAB}, \theta^3_{gyrAB})\ s^-(x_{topA}, \theta^1_{topA})\ s^+(x_{fis}, \theta^4_{fis}) - \gamma_{topA} x_{topA}. \tag{29}$$

From equation (29) we can deduce the possible synthesis and degradation rates: $M_{topA} = \{\kappa^1_{topA}, \kappa^1_{topA} + \kappa^2_{topA}\}$ and $N_{topA} = \{\gamma_{topA}\}$, respectively. As for GyrAB, we should distinguish three different threshold concentrations for TopA, θ^1_{topA}, θ^2_{topA}, and θ^3_{topA}, which are ordered in the following manner:

$$0 < \theta^1_{topA} < \theta^2_{topA} < \theta^3_{topA} < max_{topA}. \tag{30}$$

Stimulation of the *topA* promoter by DNA supercoiling and Fis allows maximal production of TopA. We therefore set $(\kappa^1_{topA} + \kappa^2_{topA})/\gamma_{topA} > \theta^3_{topA}$. In the absence of *topA* promoter stimulation, TopA is expressed at a background level. This motivates the following inequalities:

$$0 < \frac{\kappa^1_{topA}}{\gamma_{topA}} < \theta^1_{topA}, \quad \theta^3_{topA} < \frac{\kappa^1_{topA} + \kappa^2_{topA}}{\gamma_{topA}} < max_{topA}. \tag{31}$$

5.4 Stable RNA output module

In *E. coli*, the production of stable RNAs varies in proportion to the growth rate, to match the cell's changing demand for protein synthesis. Most of this regulation is achieved at the level of transcription of the seven *rrn* operons [79, 80, 99]. Stable RNAs are produced from two promoters, P1 and P2. The activity of the former is stimulated by the protein Fis, which allows a rapid bacterial growth [8, 82, 122, 123]. On the contrary, *rrn* P2 is considered a house-keeping promoter, because it is much less responsive [99] and no Fis-dependent regulation has been demonstrated. We consider that stable RNAs are produced from *rrn* P1 at a synthesis rate κ^1_{rrn} and κ^2_{rrn} from *rrn* P2. Assuming these RNAs are degraded at a constant rate $\gamma_{rrn}\ x_{rrn}$, we obtain the following state equation for stable RNAs:

$$\dot{x}_{rrn} = \kappa^1_{rrn}\ s^+(x_{fis}, \theta^3_{fis}) + \kappa^2_{rrn} - \gamma_{rrn} x_{rrn}. \tag{32}$$

Analysis of equation (32) shows that there are two possible synthesis rates for stable RNAs, $M_{rrn} = \{\kappa^1_{rrn}, \kappa^1_{rrn} + \kappa^2_{rrn}\}$, and one degradation rate, $N_{rrn} = \{\gamma_{rrn}\}$. We distinguish a single threshold, θ_{rrn}, above which the stable RNA concentration is assumed high enough to allow bacterial growth. This leads to the straightforward threshold inequalities:

$$0 < \theta_{rrn} < max_{topA}. \tag{33}$$

We now have to order the target equilibrium values $\kappa^1_{rrn}/\gamma_{rrn}$ and $(\kappa^1_{rrn} + \kappa^2_{rrn})/\gamma_{rrn}$ with respect to the threshold values of x_{rrn}. The increase of the production of stable RNAs during exponential phase, due to the activation by Fis, implies that $(\kappa^1_{rrn} + \kappa^2_{rrn})/\gamma_{rrn} > \theta_{rrn}$. In stationary phase, these RNAs are no longer produced, which gives $\kappa^1_{rrn}/\gamma_{rrn} < \theta_{rrn}$. In summary, we have the following equilibrium inequalities:

$$0 < \frac{\kappa^1_{rrn}}{\gamma_{rrn}} < \theta_{rrn}, \quad \theta_{rrn} < \frac{\kappa^1_{rrn} + \kappa^2_{rrn}}{\gamma_{rrn}} < max_{rrn}. \tag{34}$$

$\dot{u}_s = 0$
$0 < \theta_s < max_s$

$\dot{x}_{crp} = \kappa^1_{crp} + \kappa^2_{crp}\ s^-(x_{fis}, \theta^2_{fis})\ s^+(x_{crp}, \theta^1_{crp}) s^+(x_{cya}, \theta^1_{cya})\ s^+(u_s, \theta_s) + \kappa^3_{crp}\ s^-(x_{fis}, \theta^1_{fis}) - \gamma_{crp}\ x_{crp}$
$0 < \theta^1_{crp} < \theta^2_{crp} < \theta^3_{crp} < max_{crp}$
$\theta^1_{crp} < \kappa^1_{crp}/\gamma_{crp} < \theta^2_{crp},\ \theta^1_{crp} < (\kappa^1_{crp} + \kappa^2_{crp})/\gamma_{crp} < \theta^2_{crp},\ \theta^3_{crp} < (\kappa^1_{crp} + \kappa^3_{crp})/\gamma_{crp} < max_{crp},$
$\theta^3_{crp} < (\kappa^1_{crp} + \kappa^2_{crp} + \kappa^3_{crp})/\gamma_{crp} < max_{crp}$

$\dot{x}_{cya} = \kappa^1_{cya} + \kappa^2_{cya}\ (1 - s^+(x_{crp}, \theta^3_{crp})\ s^+(x_{cya}, \theta^3_{cya})\ s^+(u_s, \theta_s)) - \gamma_{cya}\ x_{cya}$
$0 < \theta^1_{cya} < \theta^2_{cya} < \theta^3_{cya} < max_{cya}$
$\theta^1_{cya} < \kappa^1_{cya}/\gamma_{cya} < \theta^2_{cya},\ \theta^3_{cya} < (\kappa^1_{cya} + \kappa^2_{cya})/\gamma_{cya} < max_{cya}$

$\dot{x}_{fis} = \kappa^1_{fis}\ (1 - s^+(x_{crp}, \theta^1_{crp})\ s^+(x_{cya}, \theta^1_{cya})\ s^+(u_s, \theta_s))\ s^-(x_{fis}, \theta^5_{fis})$
$\quad + \kappa^2_{fis}\ s^+(x_{gyrAB}, \theta^2_{gyrAB})\ s^-(x_{topA}, \theta^2_{topA})\ s^-(x_{fis}, \theta^5_{fis})\ (1 - s^+(x_{crp}, \theta^1_{crp})\ s^+(x_{cya}, \theta^1_{cya})\ s^+(u_s, \theta_s)) - \gamma_{fis}\ x_{fis}$
$0 < \theta^1_{fis} < \theta^2_{fis} < \theta^3_{fis} < \theta^4_{fis} < \theta^5_{fis} < max_{fis}$
$\theta^1_{fis} < \kappa^1_{fis}/\gamma_{fis} < \theta^2_{fis},\ \theta^5_{fis} < (\kappa^1_{fis} + \kappa^2_{fis})/\gamma_{fis} < max_{fis}$

$\dot{x}_{gyrAB} = \kappa^1_{gyrAB} + \kappa^2_{gyrAB}\ (1 - s^+(x_{gyrAB}, \theta^3_{gyrAB})\ s^-(x_{topA}, \theta^1_{topA}))\ s^-(x_{fis}, \theta^4_{fis}) - \gamma_{gyrAB}\ x_{gyrAB}$
$0 < \theta^1_{gyrAB} < \theta^2_{gyrAB} < \theta^3_{gyrAB} < max_{gyrAB}$
$0 < \kappa^1_{gyrAB}/\gamma_{gyrAB} < \theta^1_{gyrAB},\ \theta^3_{gyrAB} < (\kappa^1_{gyrAB} + \kappa^2_{gyrAB})/\gamma_{gyrAB} < max_{gyrAB}$

$\dot{x}_{topA} = \kappa^1_{topA} + \kappa^2_{topA}\ s^+(x_{gyrAB}, \theta^3_{gyrAB})\ s^-(x_{topA}, \theta^1_{topA})\ s^+(x_{fis}, \theta^4_{fis}) - \gamma_{topA}\ x_{topA}$
$0 < \theta^1_{topA} < \theta^2_{topA} < \theta^3_{topA} < max_{topA}$
$0 < \kappa^1_{topA}/\gamma_{topA} < \theta^1_{topA},\ \theta^3_{topA} < (\kappa^1_{topA} + \kappa^2_{topA})/\gamma_{topA} < max_{topA}$

$\dot{x}_{rrn} = \kappa^1_{rrn}\ s^+(x_{fis}, \theta^3_{fis}) + \kappa^2_{rrn} - \gamma_{rrn}\ x_{rrn}$
$0 < \theta_{rrn} < max_{topA}$
$0 < \kappa^1_{rrn}/\gamma_{rrn} < \theta_{rrn},\ \theta_{rrn} < (\kappa^1_{rrn} + \kappa^2_{rrn})/\gamma_{rrn} < max_{rrn}$

Figure 11: State equations and parameters inequalities for the nutritional stress response network in figure 2. The model has six state variables corresponding to the concentrations of key proteins or RNAs, and one exogenous variable denoting the presence of a nutritional stress signal: x_{crp} (CRP), x_{Cya} (Cya), x_{fis} (Fis), x_{gyrAB} (GyrAB), x_{topA} (TopA), x_{rrn} (stable RNAs), x_s (Signal).

6 Simulation of nutritional stress response

The model presented in the previous section consists of 6 state variables, one input variable, 19 threshold parameters, and 19 rate parameters. In addition, we have specified 54 threshold and equilibrium inequalities. The choice for particular regulation functions and parameters inequalities was motivated by the available genetic and molecular data about the nutritional stress response in *E. coli*. Using the model, we simulate in this section the response of the bacterium to the absence or presence of nutrients in the growth medium. The simulations lead to qualitative behavioral predictions that can be compared with experimental observations reported in the literature. All simulations described below have been carried out by means of the computer tool GNA (section 3).

In section 6.1, we simulate the transition of *E. coli* from exponential to stationary phase in response to a nutrient deprivation. In agreement with biological data, the propagation of the nutritional stress signal through the network leads to the adaptation of cellular growth. However, the DNA supercoiling level is not adjusted, which is inconsistent with published data and suggests new experiments. In section 6.2, we simulate the transition of *E. coli* from stationary to exponential phase in response to a nutrient upshift. Bacterial growth indeed adapts to the sudden availability of nutrients, but does so in an unexpected way, through damped oscillations towards a new equilibrium value of the concentrations of some of the network components. Interestingly, this observation has never been reported in the literature, although some early studies suggest this possibility. A close examination of the nutritional stress response network gives an explanation of how the damped oscillations emerge from the interactions between the network components.

6.1 Simulation of the entry into stationary phase

E. coli cells grow exponentially in a fresh growth medium, until an essential nutrient is depleted, obliging cells to slow down their growth and enter stationary phase. The adaptation of the cells to the changing nutrient conditions relies on the intricate network of interactions between the global regulators of the bacterium (figure 2). The nutritional stress signal acts on this network through the activation of the adenylate cyclase, Cya, and the subsequent formation of the cAMP·CRP complex.

In the absence of the nutritional stress signal ($0 \leq u_s < \theta_s$), the system reaches a single qualitative equilibrium state (section 6.2), associated with the following switching domain

$$\begin{array}{ll} \theta^1_{crp} < x_{crp} < \theta^2_{crp}, & \theta^3_{cya} < x_{cya} \leq max_{cya}, \\ x_{fis} = \theta^4_{fis}, & x_{gyrAB} = \theta^2_{gyrAB}, \\ 0 \leq x_{topA} < \theta^1_{topA}, & \theta^1_{rrn} < x_{rrn} \leq max_{rrn}, \\ 0 \leq u_s < \theta_s. & \end{array} \tag{35}$$

This state is consistent with physiological conditions found in exponentially-growing cells. In fact, in the course of the exponential phase, *E. coli* cells have been shown to contain a low concentration of CRP [53], while the level of Cya [97], Fis [6, 10, 89], and DNA supercoiling [9] is high.

Starting from this qualitative equilibrium state, we perturb the system by switching on the nutritional stress signal ($\theta_s < u_s < max_s$). Simulation of the network takes less than one second to complete on a PC (2.4 GHz, 512 Mb) and gives rise to a transition graph of 128 qualitative states. Many of these states are associated with switching domains that the system traverses instantaneously. Since the biological relevance of the latter states is limited, they can be eliminated. This leads to a reduced transition graph of 22 qualitative states. The state transition graph contains a single qualitative equilibrium state that the system eventually reaches in all qualitative behaviors.

A typical qualitative behavior is shown in figure 12. The system starts from a qualitative equilibrium state, corresponding to exponential-phase conditions, to reach another qualitative equilibrium state corresponding to the physiological conditions found in stationary phase (see below). The first event

after receiving the nutritional stress signal is the decrease of the Fis concentration. As a consequence, the level of stable RNAs starts to decrease as well. The next event concerns the increase of the CRP concentration, followed by a decrease of the level of Cya. In parallel, the concentration of GyrAB increases, whereas the concentration of TopA remains constant, which causes the level of DNA supercoiling to rise.

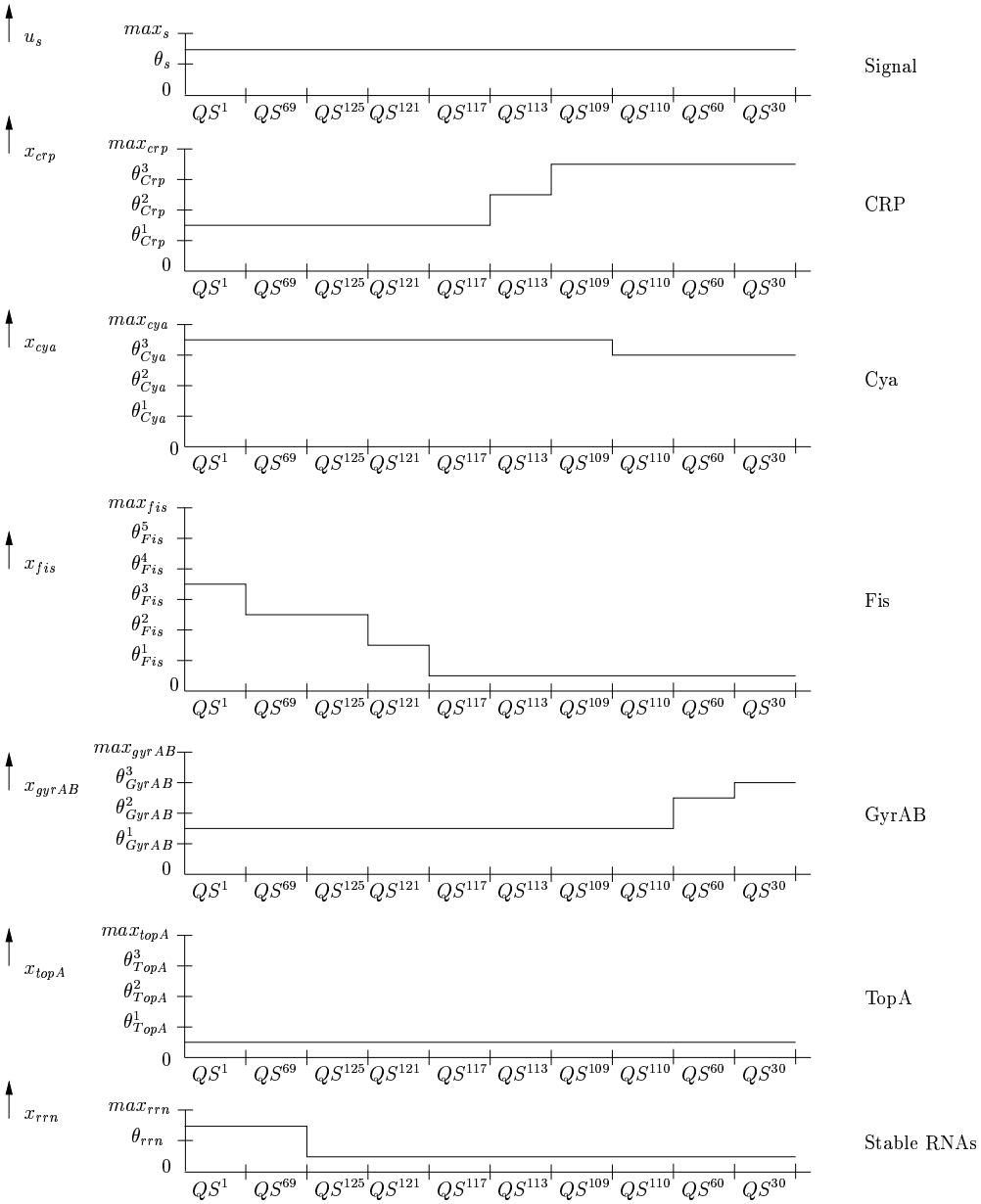

Figure 12: Temporal evolution of the protein or RNA concentrations in a typical qualitative behavior in the state transition graph, when Signal is present ($\theta_s < u_s < max_s$). The behavior represents the molecular events accompanying the transition from exponential to stationary phase.

As explained in section 2, the concentration of the stable RNAs is a good indicator of the cell's growth state. Whereas cells in exponential phase need massive amounts of RNA for the translation of the proteins, a low concentration of the stable RNAs is sufficient for the reduced activity of the translation machinery in stationary phase [16, 61]. Since the level of RNAs is low in the qualitative equilibrium state reached by the system after a nutritional stress signal, we conclude that this state is representative for a stationary-phase cell. The process driving the cell's growth arrest can be explained

by relating the qualitative behavior to the nutritional stress response network in figure 2. During exponential phase, the adenylate cyclase is present, but inactive. When the nutritional stress signal is switched on, it activates the protein and thus enables it to produce cAMP. The metabolite binds to CRP, which is not yet abundant, thus giving rise to a low concentration of the cAMP·CRP complex. The level of cAMP·CRP is nevertheless high enough to start repressing the expression of *fis*. This stimulates further accumulation of CRP, and thus further repression of Fis, through the derepression of the Fis-controlled promoters of *crp*. The decrease of the Fis concentration also causes the downregulation of the expression of the *rrn* genes. As a consequence, the level of the stable RNAs decreases and the cell enters stationary phase.

We conclude from our model of the nutritional stress response network that a positive feedback mechanism, the mutual inhibition of *fis* and *crp*, plays a key role in the transition from exponential phase to stationary phase. In the presence of a nutritional stress, it causes a switch from a state in which Fis is high and CRP low to a state in which Fis is low and CRP high. The predicted evolution of the Fis concentration is in agreement with experimental data [6, 10, 89] showing a 50-fold decrease of the level of this protein when going from exponential to stationary phase. Unfortunately, equally-precise measurements are not available for CRP, although available evidence tends to confirm the model predictions. Whereas the protein has been shown to accumulate to low concentrations in the presence of glucose, that is, under conditions of exponential growth, a high concentration is observed when glucose is absent (which is the case under stationary-phase conditions [53]).

The predicted qualitative evolution of the protein concentrations in figure 12 implies that the DNA supercoiling level increases at the onset of stationary phase. In fact, the production of the cAMP·CRP complex in response to the nutritional stress signal causes the concentration of Fis to decrease, as explained above. As a consequence, the protein can no longer repress the expression of GyrAB, whose concentration starts to increase. Given that the concentration of TopA remains low, this means that the DNA supercoiling level increases. However, this is not what has been observed experimentally. On the contrary, the DNA supercoiling level has been shown to decrease when *E. coli* cells enter stationary phase [9]. The inconsistency between the predicted and observed level of supercoiling suggests that our picture of the nutritional stress response network is incomplete, in the sense that interactions between the global regulators in figure 2, or additional regulators not shown in the figure, are missing. In section 7, we propose experiments and model extensions to further investigate these possibilities.

6.2 Simulation of the reentry into exponential phase

When cells in stationary phase are put into fresh medium, the consequent nutrient upshift causes them to reenter exponential phase. Information on this nutrient recovery is transmitted to the nutritional stress response network through the deactivation of the adenylate cyclase, Cya, which stops the formation of the cAMP·CRP complex.

In order to simulate the above transition from stationary to exponential phase, we use the qualitative equilibrium state reached under stationary-phase conditions (section 6.1) as the initial qualitative state, except for the adjustment of GyrAB to obtain the observed low level of supercoiling:

$$\begin{array}{ll} \theta^3_{crp} < x_{crp} \leq max_{crp}, & x_{cya} = \theta^3_{cya}, \\ 0 \leq x_{fis} < \theta^1_{fis}, & 0 \leq x_{gyrAB} < \theta^1_{gyrAB}, \\ 0 \leq x_{topA} < \theta^1_{topA}, & 0 \leq x_{rrn} < \theta_{rrn}, \\ \theta_s < u_s < max_s. & \end{array} \tag{36}$$

Starting from this state, we perturb the system by switching off the nutritional stress signal ($0 \leq u_s < \theta_s$). Simulation of the network takes less than one second to complete and gives rise to a transition graph of 642 qualitative states. Elimination of the instantaneous states leads to a reduced transition graph of 75 qualitative states. Unexpectedly, all qualitative behaviors in the graph are attracted by a qualitative cycle.

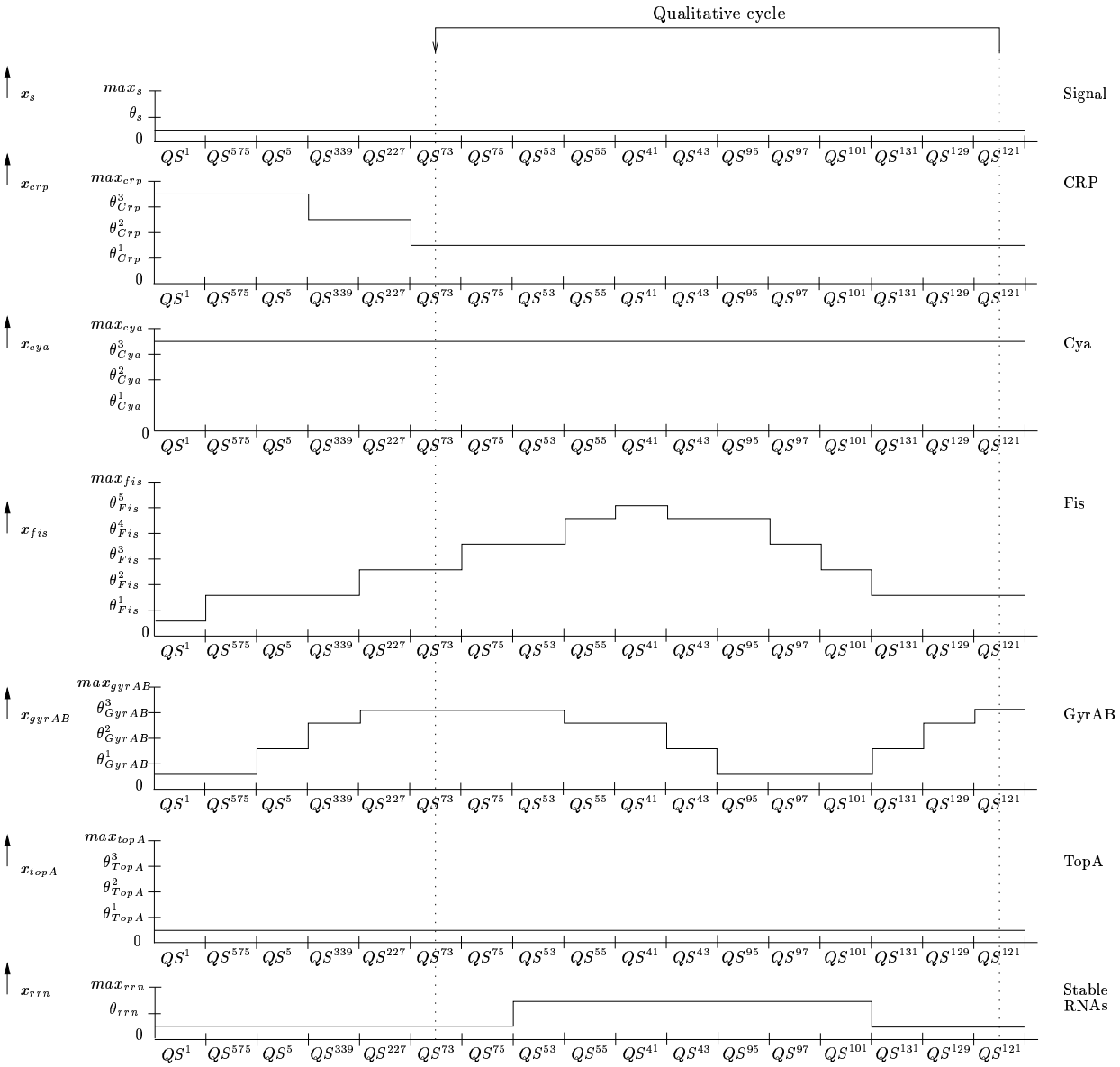

Figure 13: Temporal evolution of the protein or RNA concentrations in a typical qualitative behavior in the state transition graph, when Signal is absent ($0 \leq u_s < \theta_s$). The behavior represents the molecular events accompanying the transition from stationary to exponential phase.

A typical qualitative behavior leading to the qualitative cycle is shown in figure 13. After the nutritional stress signal is switched off, an increase of the Fis concentration is predicted, followed by a decrease of the CRP concentration, the exact opposite of what is seen in figure 12. The system then enters the qualitative cycle. Whereas the concentrations of CRP, Cya, and TopA remain constant along the cycle, the concentrations of Fis, GyrAB, and the stable RNAs oscillate. In particular, the GyrAB level starts to decrease, followed by the decrease of the level of Fis and, consequently, of the stable RNAs. The level of GyrAB then rises again, followed by increases of the levels of Fis and stable RNAs, which completes the qualitative cycle.

The information in the state transition graph is not sufficient to decide whether the qualitative cycle in figure 13 corresponds to a limit cycle or to trajectories spiralling towards an equilibrium point. However, a more detailed analysis (J.L. Gouzé, personal communication) has shown that, for all parameters values satisfying the inequality constraints, the qualitative cycle corresponds to the second possibility, that is, to a damped oscillation towards an equilibrium point. The latter equilibrium point is located in the switching domain (35), associated with a qualitative equilibrium state in the transition graph.

As explained in section 6.1, the qualitative equilibrium state is representative for the physiology of an *E. coli* cell in exponential phase. That is, CRP is present in the cell at a low concentration, while the concentration of Cya is maximal and the concentration of Fis and the DNA supercoiling level are at intermediate values. The occurrence of damped oscillations in response to a nutrient upshift is an unexpected result of the simulation. However, the oscillations can be easily explained by looking at the regulatory interactions between Fis, GyrAB, and TopA in figure 2. The deactivation of Cya, following the switching-off of the nutrient-stress signal, stops the production of cAMP·CRP and leads to a reversal of the fates of the CRP and Fis concentrations: Fis starts to accumulate, whereas CRP degrades. The increase of the Fis concentration activates the expression of *topA* and represses the expression of *gyrAB*, thereby lowering the DNA supercoiling level. This causes *fis* transcription from the P promoter to slow down, which restores GyrAB expression and inhibits TopA expression, thus increasing the negative supercoiling again. As a consequence, *fis* expression is stimulated, thus finishing the first period of the Fis-supercoiling oscillations. Due to the regulation of the *rrn* genes by Fis, the concentration of the stable RNAs oscillate as well.

The predicted damped oscillations in the concentrations of Fis and GyrAB after a nutrient upshift arise from the negative feedback loops relating these proteins and TopA. Currently, no experimental data is available that would allow the oscillation of the components of this homeostatic control mechanism to be confirmed. Some indirect evidence is provided by pulse-chase labelling measurements of the concentrations of ribosomal proteins and their messenger RNAs, stable RNAs, and total RNAs [32, 33, 121]. Indeed, damped oscillations towards a higher equilibrium level have been observed until one hour after a nutrient upshift. This conforts the idea of the oscillatory behavior of the other proteins, and calls for measurements of the concentrations of Fis, GyrAB, and TopA immediately following a nutrient upshift (section 7).

7 Discussion

In this report, we have modeled and simulated the genetic regulatory network controlling the nutritional stress response in *E. coli*. We have first constructed the nutritional stress response network by identifying key global regulators involved in the process (section 2). Since quantitative information on the values of the kinetic parameters and molecular concentrations is lacking in most cases, we have chosen a qualitative modeling and simulation method to analyze the network. This method is based on a class of piecewise-linear differential equations, using step functions to describe the regulatory mechanisms (section 3). The step functions are approximations of sigmoidal functions that describe the often complex regulatory mechanisms involved in gene regulation, for instance, the effects of CRP activation by cAMP and DNA supercoiling on transcription initiation (section 4). By integrating the available

experimental data about the regulatory mechanisms underlying the interactions, we have developed a model of six piecewise-linear differential equations describing the nutritional stress response network (section 5). Instead of assigning numerical values to the kinetic parameters, about fifty constraints in the form of algebraic inequalities have been obtained from the experimental literature.

Using this model, we have simulated the nutrient stress response of *E. coli* cells by means of the computer tool GNA, and the simulation results have been compared with experimental data. The model predictions have led to new insights into how *E. coli* performs its growth transitions in response to changes in the nutrient conditions (section 6). In particular, the model suggests that the mutual inhibition of Fis and CRP plays a determining role in the transition from exponential to stationary phase. In addition, the inconsistency between the predicted and observed evolution of the DNA supercoiling level during this growth-phase transition indicates that the nutritional stress response network is incomplete, in the sense that certain interactions or global regulators involved in the control of DNA supercoiling are missing. The model also predicts that, in response to a nutrient upshift, the concentrations of the key proteins Fis and GyrAB display damped oscillations towards a new equilibrium, representative of exponential-phase conditions. This surprising behavior, which has not been experimentally verified thus far, is a direct consequence of the homeostatic control of the DNA-supercoiling level.

The mutual inhibition of Fis and CRP is a paradigm case of positive feedback, a control mechanism known to play a key role in developmental processes [110]. In response to a perturbation, it may cause the system to switch from one equilibrium to another, for instance, from a state with a high Fis concentration and a low CRP concentration to a state with a low Fis concentration and a high CRP concentration. This switching behavior is a crucial property for cellular differentiation. Mechanisms similar to the mutual inhibition of Fis and CRP have been described for other bacterial stress responses. The best-known example is probably the one consisting of the genes *cI* and *cro* of the bacteriophage λ [90], that are involved in the switch between the lytic and lysogenic states of infected *E. coli* cells.

The conflict between the observed and predicted levels of DNA supercoiling in section 6.1 illustrates an important function of a model: it reveals the incompleteness of the information taken into account to explain a phenomenon, and suggests ways to complete it. How can we adapt the model so as to predict a decrease instead of an increase in the concentration of GyrAB during the transition to stationary phase? One way to extend the model would be to include an interaction regulating the transcription of *gyrAB*, for instance the inhibition of this gene by cAMP·CRP. This interaction prevents GyrAB from accumulating in the presence of a nutrient stress signal. It would therefore be interesting to carry out further experiments to try to establish whether there exists a physical interaction between cAMP·CRP and the promoter region of *gyrAB*. Another way to resolve the conflict is to include other global regulators, currently missing from figure 2, into the model. For instance, when adding the sigma factor RpoS, responsible for the general stress response in *E. coli* [47, 48, 46, 117], we have been able to prevent an increase in the concentration of GyrAB during the transition to stationary phase. This poses several interesting questions on the relative role of the different global regulators in the control of *gyrAB* expression, questions that we are currently addressing.

To date no direct experimental data are available to verify the occurrence of damped oscillations in the concentrations of the components Fis and GyrAB after a nutrient shift. However, the pulse-chase labelling experiments carried out in the early eighties show that the stable RNAs, under direct control of Fis, do oscillate until one hour after a nutrient upshift [32, 33, 121]. In order to extend these findings, we are carrying out measurements of the temporal evolution of the concentration of the global regulators in the stress response network in our laboratory. While granting the current absence of convincing evidence for the biological reality of the phenomenon, one could nevertheless speculate as to the function of these damped oscillations. A possible explanation could be given by extrapolating the conclusions of a recent article on the role of negative feedback loops in the speed-up of cellular response times [94]. The homeostatic mechanism involving Fis and the proteins regulating the super-

coiling level introduces a delay in the negative feedback loop. This speeds up the adaptation of the cell to the sudden availability of nutrients, by adjusting the concentrations of Fis and GyrAB to a new equilibrium level. However, because the delayed feedback causes an overshoot when the concentrations approach their new equilibrium level, oscillations arise.

The results presented in this report show that the qualitative modeling and simulation of the nutritional stress response in *E. coli* has allowed us to gain a comprehension of how this process emerges from a complex network of molecular interactions. Moreover, the use of qualitative modeling and simulation has motivated concrete, well-defined experiments to test certain aspects of our understanding of the system. More generally, the results of our work suggest that qualitative methods for the analysis of genetic regulatory networks extend the application of modeling and simulation tools to systems for which precise knowledge on regulatory mechanisms and quantitative information on parameter values is absent. As is well-known, this is the case for the majority of systems studied by experimental biologists today.

Acknowledgments. The authors would like to thank Jean-Luc Gouzé (INRIA Sophia-Antipolis) for his contribution to this report. The authors acknowledge the financial support of the ARC GDyn initiative and the ACI IMPBio BacAttract initiative at the French Ministry for Research.

A Kinetic models of regulatory mechanisms

In this section, we present the kinetic models that were developed to describe the control of gene expression by a transcriptional regulator (section A.1), by a transcriptional regulator modified through a signal-transduction pathway (section A.2), and by the DNA supercoiling level (section A.3).

A.1 Transcriptional regulator

Consider the regulation of *rrn* by Fis in figure 4(a). Using the mass-action rate law, a detailed kinetic model of this mechanism could be developed, by taking into account the cooperative interaction of Fis and RNA polymerase, and the presence of multiple Fis-binding sites. For our purpose, it is sufficient to use the Hill rate law to describe the regulation. This law states a simple phenomenological relation between the activity of a gene and the concentration of a transcriptional regulator [34, 45]. Denoting by α_{rrn} the normalized activity of gene *fis*, $0 \leq \alpha_{rrn} \leq 1$, and by x_{fis} the concentration of Fis, the Hill function is defined as:

$$\alpha_{rrn} = \frac{x_{fis}^{\sigma}}{x_{fis}^{\sigma} + K_{fis}^{\sigma}}, \tag{37}$$

where $\sigma > 1$ is the cooperativity coefficient and K_{fis} a phenomenological constant similar to the half-saturation constant in Michaelis-Menten kinetics. The Hill function has a sigmoid shape, which corresponds to experimental observations of bacterial gene regulation [90, 118].

Even though we ignore the precise values of the parameters, using reasonable estimates, we obtain the gene activity plots in figure 5 ($K_{fis} = 5 \cdot 10^{-6} M$ and $\sigma = 3$ in (a); $K_{fis} = 10^{-5} M$ and $\sigma = 3$ in (b)). All calculations and plots have been produced using the program Matlab (MathWorks).

A.2 Transcriptional regulator activated through a signal-transduction pathway

Since cAMP·CRP stimulates transcription in a cooperative way [57], activation of the gene *crp* by the cAMP·CRP complex is described by means of the Hill rate law:

$$\alpha_{crp} = \frac{x_{crp\cdot camp}^{\sigma}}{x_{crp\cdot camp}^{\sigma} + K_{crp\cdot camp}^{\sigma}}, \tag{38}$$

where $x_{crp\cdot camp}$ and α_{crp} denote the concentration of cAMP·CRP and the normalized activity of *crp*, respectively. The constants $K_{crp\cdot camp}$ and σ have their usual meaning.

The box 'activation' in figure 6 involves the following reactions and rate constants:

$$\text{Cya*} + \text{ATP} \underset{k_{-1}}{\overset{k_1}{\rightleftarrows}} \text{Cya*} \cdot \text{ATP} \xrightarrow{k_2} \text{Cya*} + \text{cAMP} \xrightarrow{k_3} \text{Export/Degradation},$$

$$\text{cAMP} + \text{CRP} \underset{k_{-4}}{\overset{k_4}{\rightleftarrows}} \text{cAMP} \cdot \text{CRP},$$

where Cya* corresponds to the activated form of the adenylate cyclase Cya, in the presence of Signal. In addition to binding CRP, cAMP can be exported out of the cell or degraded at a rate k_3, proportional to the cAMP concentration [31, 119]. Within the cell, CRP monomers associate to form dimers with an affinity constant that is so high (10^9-10^{10} M, [42]) that the protein exists most likely only in a dimeric state in the cell. This is the reason why we do not take into account the monomeric form of CRP here.

The reactions are modeled by means of the mass-action law. Let $x_{atp\cdot free}$, $x_{camp\cdot free}$, $x_{cya\cdot free}$, $x_{crp\cdot free}$ denote the concentrations of free ATP, cAMP, Cya*, and CRP, respectively, and $x_{cya\cdot atp}$, $x_{crp\cdot camp}$ the Cya*·ATP and cAMP·CRP concentrations. Then we obtain the following system of differential equations:

$$\dot{x}_{atp\cdot free} = k_{-1}\, x_{cya\cdot atp} - k_1\, x_{atp\cdot free}\, x_{cya\cdot free}, \tag{39}$$

$$\dot{x}_{cya\cdot free} = (k_{-1} + k_2)\, x_{cya\cdot atp} - k_1\, x_{atp\cdot free}\, x_{cya\cdot free}, \tag{40}$$

$$\dot{x}_{cya\cdot atp} = k_1\, x_{cya\cdot free}\, x_{atp\cdot free} - (k_{-1} + k_2)\, x_{cya\cdot atp}, \tag{41}$$

$$\dot{x}_{camp\cdot free} = k_2\, x_{cya\cdot atp} + k_{-4}\, x_{crp\cdot camp} - k_4\, x_{crp\cdot free}\, x_{camp\cdot free} - k_3\, x_{camp\cdot free}, \tag{42}$$

$$\dot{x}_{crp\cdot free} = k_{-4}\, x_{crp\cdot camp} - k_4\, x_{crp\cdot free}\, x_{crp\cdot camp}, \tag{43}$$

$$\dot{x}_{crp\cdot camp} = k_4\, x_{crp\cdot free}\, x_{camp\cdot free} - k_{-4}\, x_{crp\cdot camp}. \tag{44}$$

In addition, we define the following conservation relations:

$$x_{crp} = x_{crp\cdot free} + x_{crp\cdot camp}, \tag{45}$$

$$x_{cya} = x_{cya\cdot free} + x_{cya\cdot atp}, \tag{46}$$

$$x_{camp} = x_{camp\cdot free} + x_{crp\cdot camp}, \tag{47}$$

$$x_{atp} = x_{atp\cdot free} + x_{cya\cdot atp}, \tag{48}$$

where x_{crp}, x_{cya}, x_{camp}, and x_{atp} denote the total cellular CRP, Cya*, cAMP, and ATP concentrations, respectively. That is, the total concentration of the proteins and metabolites equals the sum of the free and complexed concentration.

It is reasonable to assume Michaelis-Menten kinetics for the cAMP-synthesis reaction steps. However, because Cya is a low-abundant protein in the cell [119], the protein is most likely saturated by ATP and the Michaelis-Menten rate law simplifies to a pseudo-first-order rate law (see chapter 3 in [28]). This means that the production rate of cAMP from ATP, $k_2\, x_{cya\cdot atp}$, is directly proportional to the total concentration of the enzyme. More precisely,

$$k_2\, x_{cya\cdot atp} = k_2\ x_{cya}. \tag{49}$$

The conservation relations (45)-(48) and the approximation (49) allow the kinetic model (39)-(44) to be reduced to the following two differential equations:

$$\dot{x}_{camp\cdot free} = k_2\, x_{cya} + k_{-4}\, x_{crp\cdot camp} - k_4\, (x_{crp} - x_{crp\cdot camp})\, x_{camp\cdot free} - k_3\, x_{camp\cdot free}, \tag{50}$$

$$\dot{x}_{crp\cdot camp} = k_4\, (x_{crp} - x_{crp\cdot camp})\, x_{camp\cdot free} - k_{-4}\, x_{crp\cdot camp}. \tag{51}$$

Because cAMP·CRP formation is in a state of quasi-equilibrium with respect to the synthesis and degradation of proteins, as mentioned in section 4.2, we set $\dot{x}_{camp\cdot free} = 0$ and $\dot{x}_{crp\cdot camp} = 0$, and solve for $x_{crp\cdot camp}$. This gives

$$x_{crp\cdot camp} = \frac{k_2\, x_{crp}\, x_{cya}}{k_2\, x_{cya} + k_3\, K_4}, \tag{52}$$

where $K_4 = k_{-4}/k_4$. Using this equation and (38), the gene activity α_{crp} at equilibrium can be calculated.

The above derivation is valid under the condition that the signal activating adenylate cyclase is present. In the absence of Signal, the system of CRP activation is in equilibrium by definition. Since Cya synthesizes cAMP only in its activated form, we fix this equilibrium at $x_{cya} = 0$.

Based on the experimental literature, the following approximate parameter values have been chosen: $k_2 = 100$ s^{-1} [119], $k_3 = 0.035$ s^{-1} [27], $K_4 = 10^{-5}$ M [7], $K_0 = 10^{-5}$ M [26]. For the remaining parameter, we have used the value $\sigma = 3$. Calculation of the activity of *crp* as a function of the concentrations of CRP and Cya in the absence and presence of Signal, leads to the plots shown in figure 8. The sigmoidal shape of the surface is robust under moderate variation of the parameter values. The activity plots for the regulation of *fis* are obtained in the same way, with a lower value for K_0 ($2 \cdot 10^{-5}$ M).

A.3 DNA supercoiling

The regulation of *fis* in figure 9 can be modeled by means of an empirical model based on the DNA supercoiling level and the Hill rate law. The topoisomerases GyrAB and TopA ensure a fine-tuned control of the DNA supercoiling level by adding and removing negative supercoils, respectively [44]. In the absence of more precise information, we describe these antagonistic influences on the DNA supercoiling level SC by the following simple model:

$$SC = a + b\frac{x_{gyrAB}}{x_{topA}} \tag{53}$$

where x_{gyrAB} and x_{topA} denote the topoisomerase concentrations, and a and b are real positive parameters.

The DNA supercoiling level acts as a transcriptional regulator, in the sense that it may activate or inhibit initiation of transcription [44]. More precisely, measurements of the promoter activity as a function of the DNA supercoiling level have resulted in steep sigmoid curves in the physiological range. We therefore define the normalized activity of the gene *fis*, denoted by α_{fis}, as depending on the DNA supercoiling level by a Hill rate law. We obtain the following equation:

$$\alpha_{fis} = \frac{SC^\sigma}{SC^\sigma + K_{SC}^\sigma}, \tag{54}$$

where σ is the cooperativity parameter, and K_{SC} is a real constant analogous to the half-saturation constant in Michaelis-Menten kinetics. It describes the sensitivity of the *fis* promoter sequence to the DNA supercoiling level.

For arbitrary parameter values, we obtain the gene activity plots in figure 10 ($a = 0.2$, $b = 0.8$, $K_{SC} = 3$, and $\sigma = 4$ in (a); $a = 0.2$, $b = 0.8$, $K_{SC} = 3.3$, and $\sigma = 4$ in (b)). The results are robust, in the sense that moderate variations of the parameter values do not change the sigmoidal shape of the surfaces.

References

[1] T. Adachi, K. Mizuuchi, R. Menzel, and M. Gellert. DNA sequence and transcription of the region upstream of the *E. coli gyrB* gene. *Nucleic Acids Res.*, 12(16):6389–95, 1984.

[2] H. Aiba. Autoregulation of the *Escherichia coli crp* gene: CRP is a transcriptional repressor for its own gene. *Cell*, 32(1):141–9, 1983.

[3] H. Aiba. Transcription of the *Escherichia coli* adenylate cyclase gene is negatively regulated by cAMP-cAMP receptor protein. *J. Biol. Chem.*, 260(5):3063–70, 1985.

[4] H. Aiba, M. Kawamukai, and A. Ishihama. Cloning and promoter analysis of the *Escherichia coli* adenylate cyclase gene. *Nucleic Acids Res.*, 11(11):3451–65, 1983.

[5] S.E. Aiyar, S.M. McLeod, W. Ross, C.A. Hirvonen, M.S. Thomas, R.C. Johnson, and R.L. Gourse. Architecture of Fis-activated transcription complexes at the *Escherichia coli rrnB* P1 and *rrnE* P1 promoters. *J. Mol. Biol.*, 316(3):501–16, 2002.

[6] T. Ali Azam, A. Iwata, A. Nishimura, S. Ueda, and A. Ishihama. Growth phase-dependent variation in protein composition of the *Escherichia coli* nucleoid. *J. Bacteriol.*, 181(20):6361–70, 1999.

[7] W.B. Anderson, A.B. Schneider, M. Emmer, R.L. Perlman, and I. Pasta. Purification of and properties of the cyclic adenosine 3',5'-monophosphate receptor protein which mediates cyclic adenosine 3',5'-monophosphate-dependent gene transcription in *Escherichia coli. J. Biol. Chem.*, 246(19):5929–5937, 1971.

[8] J.A. Appleman, W. Ross, J. Salomon, and R.L. Gourse. Activation of *Escherichia coli* rRNA transcription by Fis during a growth cycle. *J. Bacteriol.*, 180(6):1525–32, 1998.

[9] V.L. Balke and J.D. Gralla. Changes in the linking number of supercoiled DNA accompany growth transitions in *Escherichia coli. J. Bacteriol.*, 169(10):4499–506, 1987.

[10] C.A. Ball, R. Osuna, K.C. Ferguson, and R.C. Johnson. Dramatic changes in Fis levels upon nutrient upshift in *Escherichia coli. J. Bacteriol.*, 174(24):8043–56, 1992.

[11] V.A. Bankaitis and PJ. Bassford Jr. Regulation of adenylate cyclase synthesis in *Escherichia coli*: studies with *cya-lac* operon and protein fusion strains. *J. Bacteriol.*, 151(3):1346–57, 1982.

[12] A. Barnard, A. Wolfe, and S. Busby. Regulation at complex bacterial promoters: how bacteria use different promoter organizations to produce different regulatory outcomes. *Curr. Opin. Microbiol.*, 7(2):102–8, 2004.

[13] G. Batt, D. Bergamini, H. de Jong, H. Gavarel, and R. Mateescu. Model checking genetic regulatory networks using GNA and CADP. In S. Graf and L. Mounier, editors, *Eleventh International SPIN Workshop on Model Checking of Software, SPIN 2004*, volume 2989 of *Lecture Notes in Computer Science*, pages 158–163, Berlin, 2004. Springer-Verlag.

[14] C.J. Benham. Elastic model of supercoiling. *Proc. Natl. Acad. Sci. U S A.*, 74(6):2397–401, 1977.

[15] C.J. Benham. Torsional stress and local denaturation in supercoiled DNA. *Proc. Natl. Acad. Sci. U S A.*, 76(8):3870–4, 1979.

[16] H. Bremer and P.P. Dennis. Modulation of chemical composition and other parameters of the cell by growth rate. In F.C. Neidhardt, R. Curtiss III, J.L. Ingraham, E.C.C. Lin, K.B. Low, B. Magasanik, W.S. Reznikoff, M. Riley, M. Schaechter, and H.E. Umbarger, editors, *Escherichia coli and Salmonella: Cellular and Molecular Biology*, pages 1553–69. ASM Press, Washington D.C., 1996.

[17] S. Busby and A. Kolb. The CAP modulon. In E.C.C. Lin and A.S. Lynchs, editors, *Regulation of Gene Expression in Escherichia coli*, chapter 12, pages 255–79. R.G. Landes, New-York, 1996.

[18] R. Casey, H. de Jong, and Gouzé J.-L. Piecewise-linear models of genetic regulatory networks: Equilibria and their stability. Technical Report RR-5353, INRIA, 2004.

[19] D.E. Chang, D.J. Smalley, and T. Conway. Gene expression profiling of *Escherichia coli* growth transitions: an expanded stringent response model. *Mol. Microbiol.*, 45(2):289–306, 2002.

[20] S.E. Chuang, D.L. Daniels, and F.R. Blattner. Global regulation of gene expression in *Escherichia coli*. *J. Bacteriol.*, 175(7):2026–36, 1993.

[21] H. de Jong. Modeling and simulation of genetic regulatory systems: a literature review. *J. Comput. Biol.*, 9(1):69–105, 2002.

[22] H. de Jong, J. Geiselmann, G. Batt, C. Hernandez, and M. Page. Qualitative simulation of the initiation of sporulation in *Bacillus subtilis*. *Bull. Math. Biol.*, 66(2):261–99, 2004.

[23] H. de Jong, J. Geiselmann, C. Hernandez, and M. Page. Genetic Network Analyzer: qualitative simulation of genetic regulatory networks. *Bioinformatics*, 19:336–44, 2003.

[24] H. de Jong, J.-L. Gouzé, C. Hernandez, M. Page, T. Sari, and J. Geiselmann. Qualitative simulation of genetic regulatory networks using piecewise-linear models. *Bull. Math. Biol.*, 66(2):301–40, 2004.

[25] K. Drlica. Bacterial topoisomerases and the control of DNA supercoiling. *Trends Genet.*, 6(12):433–7, 1990.

[26] R.H. Ebright, Y.W. Ebright, and A. Gunasekera. Consensus DNA site for the *Escherichia coli* catabolite gene activator protein (CAP): CAP exhibits a 450-fold higher affinity for the consensus DNA site than for the *E. coli* lac DNA site. *Nucleic Acids Res.*, 17(24):10295–305, 1989.

[27] W. Epstein, L.B. Rothman-Denes, and J. Hesse. Adenosine 3':5'-cyclic monophosphate as mediator of catabolite repression in *Escherichia coli*. *Proc. Natl. Acad. Sci. U. S. A.*, 72(6):2300–4, 1975.

[28] A. Fersht. *Enzyme Structure and Mechanism*. Freeman W.H. and Co, New York, 2nd edition, 1985.

[29] A.F. Filippov. *Differential Equations with Discontinuous Righthand Sides*. Kluwer Academic Publishers, Dordrecht, 1988.

[30] C. Francke, P.W. Postma, H.V. Westerhoff, J.G. Blom, and M.A. Peletier. Why the phosphotransferase system of *Escherichia coli* escapes diffusion limitation. *Biophys. J.*, 85(1):612–22, 2003.

[31] A.D. Fraser and H. Yamazaki. Effect of carbon sources on the rates of cyclic AMP synthesis, excretion, and degradation, and the ability to produce beta-galactosidase in *Escherichia coli*. *Can. J. Biochem.*, 57(8):1073–9, 1979.

[32] L.P. Freedman, J.M. Zengel, and L. Lindahl. Genetic dissection of stringent control and nutritional shift-up response of the *Escherichia coli* S10 ribosomal protein operon. *J. Mol. Biol.*, 185(4):701–12, 1985.

[33] K. Gausing. Regulation of ribosome biosynthesis in *E. coli*. In G. Chambliss, G.R. Graven, J. Davies, K. Davis, L. Kahan, and N. Nomura, editors, *Ribosomes: structure, function, and genetics*, pages 693–718. University Park Press, Baltimore, 1980.

[34] L. Glass and S.A. Kauffman. The logical analysis of continuous, non-linear biochemical control networks. *J. Theor. Biol.*, 39(1):103–29, 1973.

[35] G. Gonzalez-Gil, P. Bringmann, and R. Kahmann. Fis is a regulator of metabolism in *Escherichia coli*. *Mol. Microbiol.*, 22(1):21–9, 1996.

[36] G. Gonzalez-Gil, R. Kahmann, and G. Muskhelishvili. Regulation of *crp* transcription by oscillation between distinct nucleoprotein complexes. *EMBO J.*, 17(10):2877–85, 1998.

[37] G. Gosset, Z. Zhang, S. Nayyar, W.A. Cuevas, and M.H. Saier Jr. Transcriptome analysis of CRP-dependent catabolite control of gene expression in *Escherichia coli*. *J. Bacteriol.*, 186(11):3516–24, 2004.

[38] S. Gottesman. Bacterial regulation: global regulatory networks. *Annu. Rev. Genet.*, 18(18):415–41, 1984.

[39] J.-L. Gouzé and T. Sari. A class of piecewise linear differential equations arising in biological models. *Dynam. Syst.*, 17:299–316, 2003.

[40] A. Hanamura and H. Aiba. Molecular mechanism of negative autoregulation of *Escherichia coli crp* gene. *Nucleic Acids Res.*, 19(16):4413–9, 1991.

[41] A. Hanamura and H. Aiba. A new aspect of transcriptional control of the *Escherichia coli crp* gene: positive autoregulation. *Mol. Microbiol.*, 6(17):2489–97, 1992.

[42] J.G. Harman. Allosteric regulation of the cAMP receptor protein. *Biochim. Biophys. Acta.*, 1547(1):1–17, 2001.

[43] L.H. Hartwell, J.J. Hopfield, S. Leibler, and A.W. Murray. From molecular to modular cell biology. *Nature*, 402(6761):C47–52, 1999.

[44] G.W. Hatfield and C.J. Benham. DNA topology-mediated control of global gene expression in *Escherichia coli*. *Annu. Rev. Genet.*, 36:175–203, 2002.

[45] R. Heinrich and S. Schuster. *The Regulation of Cellular Systems*. Chapman and Hall, New-York, 1996.

[46] R. Hengge-Aronis. Regulation of gene expression during entry into stationary phase. In F.C. Neidhardt, R. Curtiss III, J.L. Ingraham, E.C.C. Lin, K.B. Low, B. Magasanik, W.S. Reznikoff, M. Riley, M. Schaechter, and H.E. Umbarger, editors, *Escherichia coli and Salmonella: Cellular and Molecular Biology*, pages 1497–1512. ASM Press, Washington D.C., 1996.

[47] R. Hengge-Aronis. The general stress response in *Escherichia coli*. In G. Storz and R. Hengge-Aronis, editors, *Bacterial stress responses*, pages 161–77. ASM Press, Washington D.C., 2000.

[48] R. Hengge-Aronis. Signal transduction and regulatory mechanisms involved in control of the sigma(s) (RpoS) subunit of RNA polymerase. *Microbiol. Mol. Biol. Rev.*, 66(3):373–95, 2002.

[49] C.A. Hirvonen, W. Ross, C.E. Wozniak, E. Marasco, J.R. Anthony, S.E. Aiyar, V.H. Newburn, and R.L. Gourse. Contributions of UP elements and the transcription factor Fis to expression from the seven *rrn* P1 promoters in *Escherichia coli*. *J. Bacteriol.*, 183(21):6305–14, 2001.

[50] G.W. Huisman, M.M. Siegele D.A., Zambrano, and Kolter R. Morphological and physiological changes during stationary phase. In F.C. Neidhardt, R. Curtiss III, J.L. Ingraham, E.C.C. Lin, K.B. Low, B. Magasanik, W.S. Reznikoff, M. Riley, M. Schaechter, and H.E. Umbarger, editors, *Escherichia coli and Salmonella: Cellular and Molecular Biology*, pages 1672–82. ASM Press, Washington D.C., 1996.

[51] T. Inada, H. Takahashi, T. Mizuno, and H. Aiba. Down regulation of cAMP production by cAMP receptor protein in *Escherichia coli*: an assessment of the contributions of transcriptional and posttranscriptional control of adenylate cyclase. *Mol. Gen. Genet.*, 253(1-2):198–204, 1996.

[52] A. Ishihama. Adaptation of gene expression in stationary phase bacteria. *Curr. Opin. Genet. Dev.*, 7(5):582–8, 1997.

[53] H. Ishizuka, A. Hanamura, T. Inada, and H. Aiba. Mechanism of the down-regulation of cAMP receptor protein by glucose in *Escherichia coli*: role of autoregulation of the *crp* gene. *EMBO J.*, 13(13):3077–82, 1994.

[54] H. Ishizuka, A. Hanamura, T. Kunimura, and H. Aiba. A lowered concentration of cAMP receptor protein caused by glucose is an important determinant for catabolite repression in *Escherichia coli*. *Mol. Microbiol.*, 10(2):341–50, 1993.

[55] P.R. Jensen, C.C. Van Der Weijden, L.B. Jensen, H.V. Westerhoff, and J.L. Snoep. Extensive regulation compromises the extent to which DNA gyrase controls DNA supercoiling and growth rate of *Escherichia coli*. *Eur. J. Biochem.*, 266(3):865–77, 1999.

[56] E. Joseph, C. Bernsley, N. Guiso, and A. Ullmann. Multiple regulation of the activity of adenylate cyclase in *Escherichia coli*. *Mol. Gen. Genet.*, 185(2):262–8, 1982.

[57] J.K. Joung, L.U. Le, and A. Hochschild. Synergistic activation of transcription by *Escherichia coli* cAMP receptor protein. *Proc. Natl. Acad. Sci. U. S. A.*, 90(7):3083–7, 1993.

[58] P.D. Karp, M. Arnaud, J. Collado-Vides, J. Ingraham, I.T. Paulsen, and M.H. Saier Jr. The *E. coli* EcoCyc database: no longer just a metabolic pathway database. *ASM News*, 70(1):25–30, 2004.

[59] P.D. Karp, M. Riley, M. Saier, I.T. Paulsen, J. Collado-Vides, S.M. Paley, A. Pellegrini-Toole, C. Bonavides, and S. Gama-Castro. The EcoCyc Database. *Nucleic Acids Res.*, 30(1):56–8, 2002.

[60] M. Kawamukai, J. Kishimoto, R. Utsumi, M. Himeno, T. Komano, and H. Aiba. Negative regulation of adenylate cyclase gene (*cya*) expression by cyclic AMP-cyclic AMP receptor protein in *Escherichia coli*: studies with *cya*-lac protein and operon fusion plasmids. *J. Bacteriol.*, 164(2):872–7, 1985.

[61] J. Keener and M. Nomura. Regulation of ribosome synthesis. In F.C. Neidhardt, R. Curtiss III, J.L. Ingraham, E.C.C. Lin, K.B. Low, B. Magasanik, W.S. Reznikoff, M. Riley, M. Schaechter, and H.E. Umbarger, editors, *Escherichia coli and Salmonella: Cellular and Molecular Biology*, pages 1417–31. ASM Press, Washington D.C., 1996.

[62] K.W. Kohn. Molecular interaction maps as information organizers and simulation guides. *Chaos*, 11(1):84–97, 2001.

[63] R. Kolter, D.A. Siegele, and A. Tormo. The stationary phase of the bacterial life cycle. *Annu. Rev. Microbiol.*, 47:855–74, 1993.

[64] A. Kremling, K. Bettenbrock, B. Laube, K. Jahreis, J.W. Lengeler, and E.D. Gilles. The organization of metabolic reaction networks: III. Application for diauxic growth on glucose and lactose. *Metab. Eng.*, 3(4):362–79, 2001.

[65] A. Kremling, S. Fischer, K. Sauter, T. Bettenbrock, and E.D. Gilles. Time hierarchies in the *Escherichia coli* carbohydrate uptake and metabolism. *BioSystems*, 73(1):57–71, 2004.

[66] A. Kremling and E.D. Gilles. The organization of metabolic reaction networks: II. Signal processing in hierarchical structured functional units. *Metab. Eng.*, 3(2):138–50, 2001.

[67] E. Krin, O. Sismeiro, A. Danchin, and P.N. Bertin. The regulation of enzyme IIA(Glc) expression controls adenylate cyclase activity in *Escherichia coli*. *Microbiology*, 148(5):1553–9, 2002.

[68] C.L. Lawson, D. Swigon, K.S. Murakami, S.A. Darst, H.M. Berman, and R.H. Ebright. Catabolite activator protein: DNA binding and transcription activation. *Curr. Opin. Struct. Biol.*, 14(1):10–20, 2004.

[69] M. Madan Babu and S.A. Teichmann. Evolution of transcription factors and the gene regulatory network in *Escherichia coli*. *Nucleic Acids Res.*, 31(4):1234–44, 2003.

[70] P. Mallik, T.S. Pratt, M.B. Beach, M.D. Bradley, J. Undamatla, and R. Osuna. Growth phase-dependent regulation and stringent control of *fis* are conserved processes in enteric bacteria and involve a single promoter (*fis* P) in *Escherichia coli*. *J. Bacteriol.*, 186(1):122–35, 2004.

[71] A. Martinez-Antonio and J. Collado-Vides. Identifying global regulators in transcriptional regulatory networks in bacteria. *Curr. Opin. Microbiol.*, 6(5):482–9, 2003.

[72] A.J. Bokal 4th, W. Ross, and R.L. Gourse. The transcriptional activator protein Fis: DNA interactions and cooperative interactions with RNA polymerase at the *Escherichia coli rrnB* P1 promoter. *J. Mol. Biol.*, 245(3):197–207, 1995.

[73] H.H. McAdams and A. Arkin. Simulation of prokaryotic genetic circuits. *Annu. Rev. Biophys. Biomol. Struct.*, 27:199–224, 1998.

[74] R. Menzel and M. Gellert. Regulation of the genes for *E. coli* DNA gyrase: homeostatic control of DNA supercoiling. *Cell*, 34(1):105–13, 1983.

[75] R. Menzel and Gellert M. Fusions of the *Escherichia coli gyrA* and *gyrB* control regions to the galactokinase gene are inducible by coumermycin treatment. *J. Bacteriol.*, 169(3):1272–8, 1987.

[76] R. Menzel and Gellert M. Modulation of transcription by DNA supercoiling: a deletion analysis of the *Escherichia coli gyrA* and *gyrB* promoters. *Proc. Natl. Acad. Sci. U. S. A.*, 84(12):4185–9, 1987.

[77] T. Mestl, E. Plahte, and S.W. Omholt. A mathematical framework for describing and analysing gene regulatory networks. *J. Theor. Biol.*, 176(2):291–300, 1995.

[78] K. Mori and H. Aiba. Evidence for negative control of *cya* transcription by cAMP and cAMP receptor protein in intact *Escherichia coli* cells. *J. Biol. Chem.*, 260(27):14838–43, 1985.

[79] H.D. Murray, J.A. Appleman, and R.L. Gourse. Regulation of the *Escherichia coli rrnB* P2 promoter. *J. Bacteriol.*, 185(1):28–34, 2003.

[80] H.D. Murray and R.L. Gourse. Unique roles of the *rrn* P2 rRNA promoters in *Escherichia coli*. *Mol. Microbiol.*, 52(5):1375–87, 2004.

[81] W. Nasser, M. Rochman, and G. Muskhelishvili. Transcriptional regulation of *fis* operon involves a module of multiple coupled promoters. *EMBO J.*, 21(4):715–24, 2002.

[82] L. Nilsson, H. Verbeek, E. Vijgenboom, C. van Drunen, and A. Bosch L. Vanet. Fis-dependent trans activation of stable RNA operons of *Escherichia coli* under various growth conditions. *J. Bacteriol.*, 174(3):921–9, 1992.

[83] O. Ninnemann, C. Koch, and R. Kahmann. The *E. coli fis* promoter is subject to stringent control and autoregulation. *EMBO J.*, 11(3):1075–83, 1992.

[84] K. Okamoto and M. Freundlich. Mechanism for the autogenous control of the *crp* operon: transcriptional inhibition by a divergent RNA transcript. *Proc. Natl. Acad. Sci. U. S. A.*, 83(14):5000–4, 1986.

[85] K. Okamoto, S. Hara, R. Bhasin, and M. Freundlich. Evidence *in vivo* for autogenous control of the cyclic AMP receptor protein gene (*crp*) in *Escherichia coli* by divergent RNA. *J. Bacteriol.*, 170(11):5076–9, 1988.

[86] D.E. Pettijohn. The nuleoid. In F.C. Neidhardt, R. Curtiss III, J.L. Ingraham, E.C.C. Lin, K.B. Low, B. Magasanik, W.S. Reznikoff, M. Riley, M. Schaechter, and H.E. Umbarger, editors, *Escherichia coli and Salmonella: Cellular and Molecular Biology*, pages 158–65. ASM Press, Washington D.C., 1996.

[87] E. Plahte, T. Mestl, and S.W. Omholt. A methodological basis for description and analysis of systems with complex switch-like interactions. *J. Math. Biol.*, 36:321–348, 1998.

[88] P.W. Postma, J.W. Lengeler, and G.R. Jacobson. Phosphoenolpyruvate:carbohydrate phosphotransferase systems. In F.C. Neidhardt, J.L. Curtiss III, J.L. Ingraham, E.C.C. Lin, K.B. Low, B. Magasanik, W.S. Reznikoff, M. Riley, M. Schaechter, and H.E. Umbarger, editors, *Escherichia coli and Salmonella: Cellular and Molecular Biology*, pages 1149–74. ASM Press, Washington D.C., 1996.

[89] T.S. Pratt, T. Steiner, L.S. Feldman, K.A. Walker, and R. Osuna. Deletion analysis of the *fis* promoter region in *Escherichia coli*: antagonistic effects of integration host factor and Fis. *J. Bacteriol.*, 179(20):6367–77, 1997.

[90] M. Ptashne. *A Genetic Switch: Phage λ and Higher Organisms.* Cell Press et Blackwell Science, Cambridge, MA, 1992.

[91] H. Qi, R. Menzel, and Y.C. Tse-Dinh. Regulation of *Escherichia coli topA* gene transcription: involvement of a *sigmaS*-dependent promoter. *J. Mol. Biol.*, 267(3):481–9, 1997.

[92] R.J. Reece and A. Maxwell. DNA gyrase: structure and function. *Crit. Rev. Biochem. Mol. Biol.*, 26(3-4):335–75, 1991.

[93] J.M. Rohwer, N.D. Meadow, S. Roseman, H.V. Westerhoff, and P.W. Postma. Understanding glucose transport by the bacterial phosphoenolpyruvate:glycose phosphotransferase system on the basis of kinetic measurements *in vitro*. *J. Biol. Chem.*, 275(45):34909–21, 2000.

[94] N. Rosenfeld, M.B. Elowitz, and U. Alon. Negative autoregulation speeds the response times of transcription networks. *J. Mol. Biol.*, 2002.

[95] A. Roy and A. Danchin. The *cya* locus of *Escherichia coli* K12: organization and gene products. *Mol. Gen. Genet.*, 188(3):465–71, 1982.

[96] A. Roy, C. Haziza, and A. Danchin. Regulation of adenylate cyclase synthesis in *Escherichia coli*: nucleotide sequence of the control region. *EMBO J.*, 2(5):791–7, 1983.

[97] M.H. Jr Saier, T.M. Ramseier, and Reizer J. Regulation of carbon utilization. In F.C. Neidhardt, R. Curtiss III, J.L. Ingraham, E.C.C. Lin, K.B. Low, B. Magasanik, W.S. Reznikoff, M. Riley, M. Schaechter, and H.E. Umbarger, editors, *Escherichia coli and Salmonella: Cellular and Molecular Biology*, pages 1325–43. ASM Press, Washington D.C., 1996.

[98] H. Salgado, S. Gama-Castro, A. Martinez-Antonio, E. Diaz-Peredo, F. Sanchez-Solano, M. Peralta-Gil, D. Garcia-Alonso, V. Jimenez-Jacinto, A. Santos-Zavaleta, C. Bonavides-Martinez, and J. Collado-Vides. RegulonDB (version 4.0): transcriptional regulation, operon organization and growth conditions in *Escherichia coli K-12*. *Nucleic Acids Res.*, 1(32):D303–6, 2004.

[99] D.A. Schneider, W. Ross, and R.L. Gourse. Control of rRNA expression in *Escherichia coli*. *Curr. Opin. Microbiol.*, 6(2):151–6, 2003.

[100] R. Schneider, A. Travers, T. Kutateladze, and G. Muskhelishvili. A DNA architectural protein couples cellular physiology and DNA topology in *Escherichia coli*. *Mol. Microbiol.*, 34(5):953–64, 1999.

[101] R. Schneider, A. Travers, and G. Muskhelishvili. The expression of the *Escherichia coli fis* gene is strongly dependent on the superhelical density of DNA. *Mol. Microbiol.*, 38(1):165–75, 2000.

[102] D.W. Selinger, K.J. Cheung, R. Mei, E.M. Johansson, C.S. Richmond, F.R. Blattner, D.J. Lockhart, and G.M. Church. RNA expression analysis using a 30 base pair resolution *Escherichia coli* genome array. *Nat. Biotechnol.*, 18(12):1262–8, 2000.

[103] S.S. Shen-Orr, R. Milo, S. Mangan, and U. Alon. Network motifs in the transcriptional regulation network of *Escherichia coli*. *Nat. Genet.*, 31(1):64–8, 2002.

[104] J.L. Snoep, C.C. van der Weijden, H.W. Andersen, H.V. Westerhoff, and P.R. Jensen. DNA supercoiling in *Escherichia coli* is under tight and subtle homeostatic control, involving gene-expression and metabolic regulation of both topoisomerase I and DNA gyrase. *Eur. J. Biochem.*, 269(6):1662–9, 2002.

[105] E.H. Snoussi. Qualitative dynamics of piecewise-linear differential equations: a discrete mapping approach. *Dyn. Stabil. Syst.*, 4(3-4):189–207, 1989.

[106] A.L. Sonenshein. Control of sporulation initiation in *Bacillus subtilis*. *Curr. Opin. Microbiol.*, 3(6):561–6, 2000.

[107] H. Takahashi, T. Inada, P. Postma, and H. Aiba. CRP down-regulates adenylate cyclase activity by reducing the level of phosphorylated IIA(Glc), the glucose-specific phosphotransferase protein, in *Escherichia coli*. *Mol. Gen. Genet.*, 259(3):317–26, 1998.

[108] T.H. Tani, A. Khodursky, R.M. Blumenthal, P.O. Brown, and R.G. Matthews. Adaptation to famine: a family of stationary-phase genes revealed by microarray analysis. *Proc. Natl. Acad. Sci. U. S. A.*, 99(21):13471–6, 2002.

[109] M. Thattai and B.I. Shraiman. Metabolic switching in the sugar phosphotransferase system of *Escherichia coli*. *Biophys. J.*, 85(2):744–54, 2003.

[110] R. Thomas and R. d'Ari. *Biological Feedback*. CRC Press, Boca Raton, FL, 1990.

[111] A. Travers, R. Schneider, and G. Muskhelishvili. DNA supercoiling and transcription in *Escherichia coli*: the Fis connection. *Biochimie*, 83(2):213–7, 2001.

[112] Y.C. Tse-Dinh and R.K. Beran. Multiple promoters for transcription of the *Escherichia coli* DNA topoisomerase I gene and their regulation by DNA supercoiling. *J. Mol. Biol.*, 202(4):735–42, 1988.

[113] A.U. Viretta and M. Fussenegger. Modeling the quorum sensing regulatory network of human-pathogenic *Pseudomonas aeruginosa*. *Biotechnol. Prog.*, 20(3):670–8, 2004.

[114] K.A. Walker, C.L. Atkins, and R. Osuna. Functional determinants of the *Escherichia coli fis* promoter: roles of -35, -10, and transcription initiation regions in the response to stringent control and growth phase-dependent regulation. *J. Bacteriol.*, 181(4):1269–80, 1999.

[115] J. Wang, E.D. Gilles, J.W. Lengeler, and K. Jahreis. Modeling of inducer exclusion and catabolite repression based on a PTS-dependent sucrose and non-PTS-dependent glycerol transport systems in *Escherichia coli* K-12 and its experimental verification. *J. Biotechnol.*, 92(2):133–58, 2001.

[116] D. Weinstein-Fischer, M. Elgrably-Weiss, and S. Altuvia. *Escherichia coli* response to hydrogen peroxide: a role for DNA supercoiling, topoisomerase I and Fis. *Mol. Microbiol.*, 35(6):1413–20, 2000.

[117] L.M. Wick and T. Egli. Molecular components of physiological stress responses in *Escherichia coli*. *Adv. Biochem. Eng. Biotechnol.*, 89:1–45, 2004.

[118] G. Yagil and E. Yalil. On the relation between effector concentration and the rate of induced enzyme synthesis. *Biophys. J.*, 11(1):11–27, 1971.

[119] J.K. Yang and W. Epstein. Purification and characterization of adenylate cyclase from *Escherichia coli* K12. *J. Biol. Chem.*, 258(6):3750–8, 1983.

[120] Z. Yang, Z. Haijun, and O.Y. Zhong-Can. Monte Carlo implementation of supercoiled double-stranded DNA. *Biophys. J.*, 78(4):1979–87, 2000.

[121] J.M. Zengel and L. Lindahl. Transcription of ribosomal genes during a nutritional shift-up of *Escherichia coli*. *J. Bacteriol.*, 167(3):1095–7, 1986.

[122] X. Zhang and H. Bremer. Effects of Fis on ribosome synthesis and activity and on rRNA promoter activities in *Escherichia coli*. *J. Mol. Biol.*, 259(1):27–40, 1996.

[123] X. Zhang, P. Dennis, M. Ehrenberg, and H. Bremer. Kinetic properties of *rrn* promoters in *Escherichia coli*. *Biochimie*, 54(10):981–96, 2002.

[124] H. Zhi, X. Wang, J.E. Cabrera, R.C. Johnson, and D.J. Jin. Fis stabilizes the interaction between RNA polymerase and the ribosomal promoter *rrnB* P1, leading to transcriptional activation. *J. Biol. Chem.*, 278(47):47340–9, 2003.

Unité de recherche INRIA Rhône-Alpes
655, avenue de l'Europe - 38334 Montbonnot Saint-Ismier (France)

Unité de recherche INRIA Futurs : Parc Club Orsay Université - ZAC des Vignes
4, rue Jacques Monod - 91893 ORSAY Cedex (France)
Unité de recherche INRIA Lorraine : LORIA, Technopôle de Nancy-Brabois - Campus scientifique
615, rue du Jardin Botanique - BP 101 - 54602 Villers-lès-Nancy Cedex (France)
Unité de recherche INRIA Rennes : IRISA, Campus universitaire de Beaulieu - 35042 Rennes Cedex (France)
Unité de recherche INRIA Rocquencourt : Domaine de Voluceau - Rocquencourt - BP 105 - 78153 Le Chesnay Cedex (France)
Unité de recherche INRIA Sophia Antipolis : 2004, route des Lucioles - BP 93 - 06902 Sophia Antipolis Cedex (France)

Éditeur
INRIA - Domaine de Voluceau - Rocquencourt, BP 105 - 78153 Le Chesnay Cedex (France)
http://www.inria.fr
ISSN 0249-6399